

2009

Thermal analysis of a fireplace using ANSYS

Nathaniel Michael Knop
Iowa State University

Follow this and additional works at: <https://lib.dr.iastate.edu/etd>

 Part of the [Aerospace Engineering Commons](#)

Recommended Citation

Knop, Nathaniel Michael, "Thermal analysis of a fireplace using ANSYS" (2009). *Graduate Theses and Dissertations*. 10496.
<https://lib.dr.iastate.edu/etd/10496>

This Thesis is brought to you for free and open access by the Iowa State University Capstones, Theses and Dissertations at Iowa State University Digital Repository. It has been accepted for inclusion in Graduate Theses and Dissertations by an authorized administrator of Iowa State University Digital Repository. For more information, please contact digirep@iastate.edu.

Thermal analysis of a fireplace using ANSYS

by

Nathaniel Michael Knop

A thesis submitted to the graduate faculty
in partial fulfillment of the requirements for the degree of
MASTER OF SCIENCE

Major: Aerospace Engineering

Program of Study Committee:
Vinay Dayal, Major Professor
Thomas J. Rudolphi
Michael R. Kessler

Iowa State University

Ames, Iowa

2009

Copyright © Nathaniel Michael Knop, 2009. All rights reserved.

TABLE OF CONTENTS

LIST OF TABLES	iv
LIST OF FIGURES	v
ACKNOWLEDGEMENTS	vii
ABSTRACT	viii
CHAPTER 1. Introduction	1
CHAPTER 2. Material Background	3
2.1 Heat Transfer	3
2.1.1 Conduction	3
2.1.2 Convection	3
2.1.3 Radiation	4
2.1.4 First Law of Thermodynamics	4
2.2 Fluid Flow	5
2.2.1 Continuity Equation	5
2.2.2 Navier-Stokes Equations	5
2.2.3 Energy Equation	7
2.3 Finite Element Method	7
2.3.1 Discretize the Domain	7
2.3.2 Develop Shape Functions	8
CHAPTER 3. Design	10
3.1 Simplification	10
3.1.1 Removing Unnecessary Geometries	11

3.1.2	Remodeling the Ducts	12
3.1.3	Increasing the Wall Thickness	13
3.2	Design in ANSYS	15
3.3	Choosing Element Type	16
3.4	Materials	17
3.4.1	Aluminized Steel and Galvanized Steel	17
3.4.2	Fiber Refractory	17
3.4.3	Tempered Glass	18
3.4.4	Air	18
CHAPTER 4. Results		20
4.1	Thickness Study	20
4.2	Example 1	24
4.2.1	Example 1 Results	26
4.3	Example 2	30
4.3.1	Example 2 Results	32
4.4	2-dimensional Fireplace	37
4.5	Results	40
CHAPTER 5. Conclusions		48
BIBLIOGRAPHY		49

LIST OF TABLES

Table 3.1	Thermal properties of aluminized and galvanized steel	18
Table 4.1	Thermal properties of aluminum walls of varying thickness	20
Table 4.2	Thermal properties of air	21
Table 4.3	Temperature along the horizontal centerline	24
Table 4.4	Thermal properties for Example 1	26

LIST OF FIGURES

Figure 2.1	Discretized control volume	8
Figure 2.2	1-dimensional linear element	8
Figure 3.1	Simplification of the fireplace outer shell	12
Figure 3.2	Equivalent square duct	13
Figure 3.3	Fireplace model in ANSYS	16
Figure 4.1	Setup for thickness analysis	21
Figure 4.2	Meshing with 30 elements/line	22
Figure 4.3	Temperature contour for each solid area	22
Figure 4.4	Pressure and velocity vector contours	23
Figure 4.5	Temperature over time for varying wall thickness	23
Figure 4.6	Setup for Example 1	25
Figure 4.7	Example 1 temperature contour plot	27
Figure 4.8	Example 1 pressure contour plot	27
Figure 4.9	Example 1 velocity contour and vector plots	28
Figure 4.10	Example 1 density contour plot	28
Figure 4.11	Conditions at the outlet	30
Figure 4.12	Setup for Example 2	31
Figure 4.13	Temperature contour for Example 2	32
Figure 4.14	Pressure contour for Example 2	33
Figure 4.15	Velocity contour for Example 2	33
Figure 4.16	Density contour for Example 2	35

Figure 4.17	Temperature and pressure contour closeup for Example 2	35
Figure 4.18	Velocity contour and vector closeup for Example 2	36
Figure 4.19	Density contour closeup for Example 2	36
Figure 4.20	Obtaining the 2-dimensional cross-section	37
Figure 4.21	Setup for 2-d fireplace analysis	38
Figure 4.22	Poor inlet air flow model resulting from conversion to 2-dimensions . . .	39
Figure 4.23	Incorrect air flow path resulting from conversion to 2-dimensions . . .	40
Figure 4.24	2-dimensional fireplace temperature contour plot	41
Figure 4.25	2-dimensional fireplace pressure contour plot	42
Figure 4.26	2-dimensional fireplace density contour plot	42
Figure 4.27	Temperature contour plot inside the fireplace	43
Figure 4.28	Velocity solution inside the fireplace	44
Figure 4.29	Density contour plot inside of the fireplace	44
Figure 4.30	Temperature comparison of the inner glass (1000°F)	45
Figure 4.31	Temperature comparison of the inner glass (3600°F)	46
Figure 4.32	Flame locations for the fireplace burner pan	47

ACKNOWLEDGEMENTS

I would like to thank my major professor, Dr. Vinay Dayal, for his expertise and guidance in ANSYS. Without his help this would have been an overwhelming task. I would also like to thank Dr. T.J. Rudolphi, whom has provided much knowledge and help in understanding the Finite Element method and its' applications, and Dr. Tom Shih, whose knowledge of Computational Fluid Dynamics is unparalleled, and whom helped a great deal when modeling the flow through this fireplace. These gentlemen have always made themselves available to me and without their help I would not be where I am today.

ABSTRACT

The Finite Element analysis of a fireplace using ANSYS is presented in this document, along with the steps which have led up to its final design. The intention of this analysis is to determine the feasibility of moving from an experimentation oriented design process, where different prototypes in a fireplace's design stage are built, operated, and analyzed over the course of many months to determine an optimum design for the fireplace, to an analytical design process, where the majority of the design work is done using computer software. By making this move from experimental methods to analytical methods, a manufacturer can expect to save both time and money.

First, a brief introduction to the basics of heat transfer and fluid flow are presented to introduce the reader to some of the terminology that will be used in this document, along with some general information about the fireplace model being presented. The analysis and results are then presented starting from initial testing to determine the effects of varying thickness on a materials thermal response, continuing to initial simplified designs of the fireplace and determining boundary conditions, and ending with the full 2-dimensional transient analysis and solution of the fireplace with comparisons made to experimental data provided for this particular fireplace.

CHAPTER 1. Introduction

Finite element analysis (FEA) is a method that is being used more and more in industry to simulate structures and the loads that act on them. This method allows companies to foresee how a product will respond in real-time situations before they actually begin the construction of that product. As a result, they are able to alter their designs or materials using a limited number of prototype stages. This saves money both in the cost of materials as well as in the time taken in construction and real time testing.

The research presented in this document is concerned with the development and thermal analysis of a gas powered fireplace using ANSYS, a finite element software. As one might guess, there are a number of standards and regulations which any producer of fireplaces must follow during the design and manufacturing process. From emissions, to temperatures, to airflow, almost every aspect of the modern fireplace is subject to certain guidelines that must be met during the design and manufacturing process. To ensure that a new product will comply with these restrictions, many companies create a series of mock fireplaces and test them in what they call a “worst-case” installation setting. Basically, they will build an entire fireplace to their current design specifications and then put it in the worst location of a room, turn it on, and then test it. One of the testing procedures, one which was simulated using ANSYS, consists of placing hundreds of thermocouples in and around the fireplace in order to measure the temperature gradient created by the fireplace when it is turned on. These values are then checked and verified to see that they fall within the acceptable ranges as mandated by the American National Standards Institute (ANSI) guidelines. If the temperature values are found to be outside of the acceptable range, the company must then alter the design of their fireplace, be it dimensions, material, shielding, etc, and then create a new mock setup

and perform the tests again. This process can take many months before a design is found that complies fully with the ANSI standards. This means extra months of financing towards re-designing, material costs, labor, as well as money lost by not releasing the fully finished product to be sold on the market. In today's global economy, the time from concept to market is extremely important and can make or break the company's market hold. If a way can be found to expedite this design process, a company stands to save a lot of money in unnecessary expenses.

In this document a working fireplace model is developed using Finite Element method. The intention of this model is to show that Finite Element analysis is a tool that can be used to accelerate the fireplace concept to market cycle. The model has been simplified so that unnecessary details do not make the model very complicated. The model is then subjected thermal and fluid loads and a thermal-fluid analysis is performed. The results of this simulation are discussed in this document.

CHAPTER 2. Material Background

2.1 Heat Transfer

Heat transfer is a method in which energy is transferred between two different bodies due to a difference in temperature between the two. There are three different modes in which this transfer of energy can take place(1):

1. Conduction
2. Convection
3. Radiation

2.1.1 Conduction

Conduction deals with the energy transfer from energetic particles to the less energetic particles surrounding it(2). This transfer of energy is quantified by Fourier's Law shown in Equation 2.1(1):

$$q_x = -k \frac{dT}{dx} \quad (2.1)$$

where: q_x = Heat flux in the x-direction

k = Thermal conductivity

T = Temperature

2.1.2 Convection

Convection heat transfer is the energy that is transferred between a solid and a moving fluid, each being at different temperatures. The rate at which this exchange of energy occurs is given by Newton's law of cooling, shown in Equation 2.2(1):

$$q = h(T_s - T_f) \quad (2.2)$$

where: q = Convective heat flux

h = Heat transfer coefficient

T_s = Temperature of the solid body

T_f = Temperature of the fluid body

2.1.3 Radiation

Thermal radiation is the energy transfer between two bodies via electromagnetic waves. This form of energy transfer is exhibit by all bodies, and requires no medium for the heat to be transferred. It can even be seen to occur in a vacuum(3). The amount of energy that can be radiated by a surface is given by the Stefan-Boltzmann law shown in Equation 2.3(1):

$$q = \epsilon\sigma T^4 \quad (2.3)$$

where: q = Radiative heat flux

ϵ = Emissivity

σ = Stefan-Boltzmann constant

T = Surface temperature of the radiating body

Here, emissivity is a measure of a material's ability to radiate energy as compared to that of a perfectly radiating black surface. This value can range from 0, a non-radiating body, to 1, a perfectly radiating black surface.

2.1.4 First Law of Thermodynamics

The first law of thermodynamics states that the energy of any system must be conserved(2). This means that the amount of energy entering a system must equal the amount of energy leaving the system. This energy balance, along with Equations 2.1-2.3, makes up the system of equations that are used to solve general heat transfer problems.

2.2 Fluid Flow

The material presented in the previous section only applies to a system consisting of solid bodies in which there is no fluid flow. For systems in which there is fluid motion present, a different set of equations must be introduced that relate to the conservation principles that must be met by a system.

2.2.1 Continuity Equation

Conservation of mass must be satisfied in any closed system. Mass must not be created or destroyed. The equation governing this principle is known as the continuity equation and is shown below in Equation 2.4:

$$\frac{\partial \rho}{\partial t} + \nabla \cdot (\rho \mathbf{V}) = 0 \quad (2.4)$$

where: ρ = Density

t = Time

∇ = Del operator = $\frac{\partial}{\partial x} \mathbf{i} + \frac{\partial}{\partial y} \mathbf{j} + \frac{\partial}{\partial z} \mathbf{k}$

\mathbf{V} = Velocity vector = $V_x \mathbf{i} + V_y \mathbf{j} + V_z \mathbf{k}$

This equation can be expanded and becomes:

$$\frac{\partial \rho}{\partial t} + \frac{\partial \rho V_x}{\partial x} + \frac{\partial \rho V_y}{\partial y} + \frac{\partial \rho V_z}{\partial z} = 0 \quad (2.5)$$

2.2.2 Navier-Stokes Equations

The Navier-Stokes equations are a collection of the 3-dimensional momentum equations for any Newtonian fluid. In fluid dynamics, a Newtonian fluid is one in which the stresses at each point in the fluid are linearly proportional to the strain rates at that point(3). These equations ensure that in any system, the momentum is conserved. This means that the total force generated by the momentum transfer in each direction must be balanced by the rate of change of momentum in each direction. The Navier-Stokes equations are provided below(6):

$$\begin{aligned}
& \frac{\partial \rho V_x}{\partial t} + \frac{\partial(\rho V_x V_x)}{\partial x} + \frac{\partial(\rho V_y V_x)}{\partial y} + \frac{\partial(\rho V_z V_x)}{\partial z} \\
= & \rho g_x - \frac{\partial P}{\partial x} + R_x + \frac{\partial}{\partial x} \left(\mu_e \frac{\partial V_x}{\partial x} \right) + \frac{\partial}{\partial y} \left(\mu_e \frac{\partial V_x}{\partial y} \right) + \frac{\partial}{\partial z} \left(\mu_e \frac{\partial V_x}{\partial z} \right) + T_x
\end{aligned} \tag{2.6}$$

$$\begin{aligned}
& \frac{\partial \rho V_y}{\partial t} + \frac{\partial(\rho V_x V_y)}{\partial x} + \frac{\partial(\rho V_y V_y)}{\partial y} + \frac{\partial(\rho V_z V_y)}{\partial z} \\
= & \rho g_y - \frac{\partial P}{\partial y} + R_y + \frac{\partial}{\partial x} \left(\mu_e \frac{\partial V_y}{\partial x} \right) + \frac{\partial}{\partial y} \left(\mu_e \frac{\partial V_y}{\partial y} \right) + \frac{\partial}{\partial z} \left(\mu_e \frac{\partial V_y}{\partial z} \right) + T_y
\end{aligned} \tag{2.7}$$

$$\begin{aligned}
& \frac{\partial \rho V_z}{\partial t} + \frac{\partial(\rho V_x V_z)}{\partial x} + \frac{\partial(\rho V_y V_z)}{\partial y} + \frac{\partial(\rho V_z V_z)}{\partial z} \\
= & \rho g_z - \frac{\partial P}{\partial z} + R_z + \frac{\partial}{\partial x} \left(\mu_e \frac{\partial V_z}{\partial x} \right) + \frac{\partial}{\partial y} \left(\mu_e \frac{\partial V_z}{\partial y} \right) + \frac{\partial}{\partial z} \left(\mu_e \frac{\partial V_z}{\partial z} \right) + T_z
\end{aligned} \tag{2.8}$$

where: $g_{x,y,z}$ = Components of acceleration due to gravity

μ_e = Effective viscosity of the fluid

$R_{x,y,z}$ = Distributed resistances

$T_{x,y,z}$ = Viscous loss terms

In Equations 2.6-2.8, the terms $R_{x,y,z}$ are inputs which the user may enter into ANSYS. These represent source terms that can be used to model things such as flow through screens or porous media. These terms are eliminated if no user-specified value is supplied. Also, the $T_{x,y,z}$ terms are eliminated in the case of incompressible flow. The final form of the Navier-Stokes equations for an incompressible flow with gravity acting in the y-direction and no distributed resistances are given in Equations 2.9-2.11.

$$\begin{aligned}
& \frac{\partial \rho V_x}{\partial t} + \frac{\partial(\rho V_x V_x)}{\partial x} + \frac{\partial(\rho V_y V_x)}{\partial y} + \frac{\partial(\rho V_z V_x)}{\partial z} \\
= & -\frac{\partial P}{\partial x} + \frac{\partial}{\partial x} \left(\mu_e \frac{\partial V_x}{\partial x} \right) + \frac{\partial}{\partial y} \left(\mu_e \frac{\partial V_x}{\partial y} \right) + \frac{\partial}{\partial z} \left(\mu_e \frac{\partial V_x}{\partial z} \right)
\end{aligned} \tag{2.9}$$

$$\begin{aligned}
& \frac{\partial \rho V_y}{\partial t} + \frac{\partial(\rho V_x V_y)}{\partial x} + \frac{\partial(\rho V_y V_y)}{\partial y} + \frac{\partial(\rho V_z V_y)}{\partial z} \\
= & \rho g_y - \frac{\partial P}{\partial y} + \frac{\partial}{\partial x} \left(\mu_e \frac{\partial V_y}{\partial x} \right) + \frac{\partial}{\partial y} \left(\mu_e \frac{\partial V_y}{\partial y} \right) + \frac{\partial}{\partial z} \left(\mu_e \frac{\partial V_y}{\partial z} \right)
\end{aligned} \tag{2.10}$$

$$\frac{\partial \rho V_z}{\partial t} + \frac{\partial(\rho V_x V_z)}{\partial x} + \frac{\partial(\rho V_y V_z)}{\partial y} + \frac{\partial(\rho V_z V_z)}{\partial z}$$

$$= -\frac{\partial P}{\partial z} + \frac{\partial}{\partial x}(\mu_e \frac{\partial V_z}{\partial x}) + \frac{\partial}{\partial y}(\mu_e \frac{\partial V_z}{\partial y}) + \frac{\partial}{\partial z}(\mu_e \frac{\partial V_z}{\partial z}) \quad (2.11)$$

2.2.3 Energy Equation

As stated before, the first law of thermodynamics requires that the energy of a system be conserved. The 3-dimensional energy equation for fluid flow is provided below(6):

$$\begin{aligned} \frac{\partial}{\partial t}(\rho C_p T) + \frac{\partial}{\partial x}(\rho v_x C_p T) + \frac{\partial}{\partial y}(\rho v_y C_p T) + \frac{\partial}{\partial z}(\rho v_z C_p T) \\ = \frac{\partial}{\partial x}(K_{xx} \frac{\partial T}{\partial x}) + \frac{\partial}{\partial y}(K_{yy} \frac{\partial T}{\partial y}) + \frac{\partial}{\partial z}(K_{zz} \frac{\partial T}{\partial z}) + Q_V \end{aligned} \quad (2.12)$$

where: ρ = Density

C_p = Specific heat

$v_{x,y,z}$ = Velocity in x,y,z directions

T = Temperature

$K_{xx,yy,zz}$ = Thermal conductivity in x,y,z directions

Q_V = Volumetric heat source

2.3 Finite Element Method

The previous section provided a brief overview of the equations which are incorporated into a Finite Element method in order to solve fluid flow problems. This section will give an introduction on how the Finite Element method can be used to solve these systems of equations.

2.3.1 Discretize the Domain

The first step involves breaking up the domain of the problem into subsections called elements. These elements can take on many different shapes such as triangles or quadrilaterals. They are characterized by a certain number of nodes which define the geometry of each of the elements. It is at these nodes that the solutionS to the fluid flow equations are found.

Figure 2.1 provides an illustration of how this procedure works. Here, a square control volume is broken up into four quadrilateral elements each with four nodes associated with them.

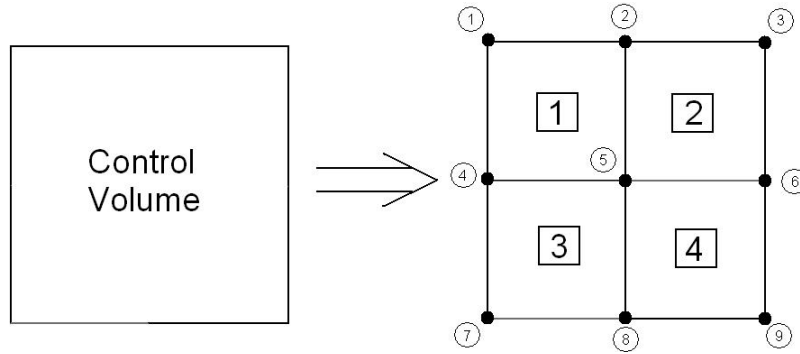


Figure 2.1 Discretized control volume

2.3.2 Develop Shape Functions

After the domain has been discretized, approximate solutions are assumed over each of the elements created. These solutions are called shape functions, or interpolation functions. They are generally quadratic functions as these are easily differentiated. In Figure 2.2, a 1-dimensional linear element is shown. Let us assume a solution for the temperature across that element can be approximated by the following linear function(1):

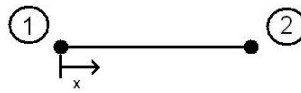


Figure 2.2 1-dimensional linear element

$$T = \alpha_1 + \alpha_2 x \quad (2.13)$$

Here, α_1 and α_2 are constants which will be solved for. Substituting the values at nodes 1 and 2 into Equation 2.13 provides:

$$T_1 = \alpha_1 + \alpha_2 x_1 \quad (2.14)$$

$$T_2 = \alpha_1 + \alpha_2 x_2 \quad (2.15)$$

From Equations 2.14-2.15, the solutions for α_1 and α_2 are found as:

$$\alpha_1 = \frac{T_1 x_2 - T_2 x_1}{x_2 - x_1} \quad (2.16)$$

$$\alpha_2 = \frac{T_2 - T_1}{x_2 - x_1} \quad (2.17)$$

Substituting these values into Equation 2.13 provides:

$$T = T_1 \left[\frac{x_2 - x}{x_2 - x_1} \right] + T_2 \left[\frac{x - x_1}{x_2 - x_1} \right] = N_1 T_1 + N_2 T_2 \quad (2.18)$$

Differentiating Equation 2.14 provides the temperature gradient across the element.

$$\frac{dT}{dx} = \frac{dN_1}{dx} T_1 + \frac{dN_2}{dx} T_2 = -\frac{1}{x_2 - x_1} T_1 + \frac{1}{x_2 - x_1} T_2 \quad (2.19)$$

Equations 2.18-2.19 define the approximated temperature and temperature gradient across the entire element. For a system of many elements and nodes, this process is done iteratively, with shape functions being applied to each element in the system. From here a system of matrices is developed to put the entire system of equations into a form shown in Equation 2.20.

$$[K]\{T\} = \{f\} \quad (2.20)$$

Where $[K]$ can be thought of as the collection of all the coefficients of $\{T\}$. $\{T\}$ is the collection of unknown terms, in this case the nodal temperatures and temperature gradients, and $\{f\}$ is the collection of known values of the system. This system of equations is then solved and the nodal values for the dependent variables in $\{T\}$ are found.

CHAPTER 3. Design

The design for the fireplace presented in this research was provided by one of the largest manufacturers and distributors in the world. Schematics for virtually every component making up the fireplace were supplied and it is understood that no changes to the current design were to be made unless specified by the manufacturer. The fireplace model supplied was developed in Pro Engineering, a computer-aided-drawing (CAD) software, and had to be converted into a type usable by ANSYS. In most cases, models created in ProE are directly compatible with ANSYS and the conversion between the two is a very smooth process. This was not the case when attempting to convert the fireplace drawings. The fireplace is a very complex structure with many intricate features that make analysis using ANSYS a difficult to near impossible task. Therefore, before the modeling in ANSYS could be started, the current ProE model had to be simplified.

3.1 Simplification

The first task when modeling the fireplace in ANSYS was to try and simplify the model and reduce the number of nodes and elements required to mesh it. In order to solve a model in ANSYS, the user must first create a mesh. This process breaks the model up into differential volumes or areas, depending on how many dimensions are being used. Each of these differential volumes and areas has nodes associated with them that determine the elements geometry and location. It is at these nodes that ANSYS solves the various conservation equations. This means that a model requiring a large number of elements and nodes to mesh it will also require a large system of equations to be solved. With an increased system of equations also comes a longer time to solution so there is much to gain by simplifying the geometry of the

model. Also, some versions of ANSYS limit the total number of elements and nodes the user is allowed to create and solving some models could be nearly impossible without simplification.

Modeling is made even more difficult due to the fact that this fireplace is a very thin-bodied structure. Most of the components of this fireplace have thickness around 0.021”-0.03” while the largest dimension is on the order of 40”. Element sizing becomes very difficult when dealing with thin bodies such as this. In Finite Element technique, the element dimensions should be similar in size to ensure that the calculations performed will be as accurate as possible. With this structure having very thin walls, the ability to keep these element lengths similar in size becomes a very difficult task. Much care must be taken when meshing the structure with particular attention paid to areas of small thickness.

3.1.1 Removing Unnecessary Geometries

Many options are available when attempting to simplify a CAD model. One obvious solution is removing parts of a model that will have a negligible effect overall when performing an analysis. This includes fasteners such as screws and the screw holes associated with them, brackets and plates used for attaching sections to each other and any other devices used for securing one section of the fireplace to another. All points of connection are assumed to be air tight and the separate pieces can be considered as one continuous component. Also, a number of dimples and bumps can be seen on the surfaces of the fireplace. These will provide little to no effect when performing an analysis and have been disregarded when modeling in ANSYS. All surfaces are considered to be smooth and continuous. A sample of a simplified component can be seen in Figure 3.1. Here, various holes and mounting brackets have been removed as well as the duct cover on the top of the unit. The simulations that have been performed were done with a top vented fireplace model which is the reason for the vent hole on the top of the unit as opposed to the back of the unit which is depicted in the left picture. The holes that can be seen on the sides of the outer shell are where controls would be housed on the actual fireplace. These are assumed to have air tight seals and have been removed when modeling the fireplace in ANSYS.

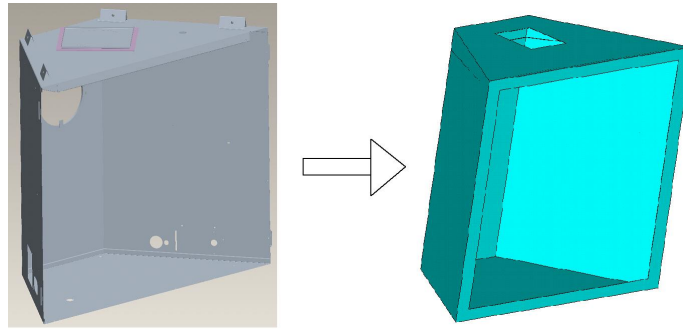


Figure 3.1 Simplification of the fireplace outer shell

The burner itself was also neglected when creating the ANSYS model. It was instead replaced by a source of heat whose energy output can be specified by the user. This number is dictated by the model of fireplace being designed and is set to reflect the total amount of heat, in BTUs, that is generated by the burner.

3.1.2 Remodeling the Ducts

Another simplification made to the model pertains to the ducts which vent out air from the inner fireplace as well as allow ambient air to flow into the burner for combustion. For these ducts, aluminum sheets are rolled to create a cylindrical column that air can pass through. Shapes such as cylinders can cause difficulties in ANSYS when meshing because it is hard to approximate a curved surface with a straight line even when controlling element sizing. To solve this problem, the ducts were modeled as boxes with cross-sectional areas identical to the cylindrical ones. This simplifies the task of modeling and also uses fewer elements when meshing, allowing for a more refined mesh overall. Care has been taken to ensure the same amount of air is allowed to pass through the square ducts as in the circular ones. This is satisfied by calculating the cross-sectional areas for both the inner and outer volumes of air in the ducts and then calculating the dimensions of the square ducts that give the same cross-

sectional areas. A sample calculation is shown below using the ducts shown in Figure 3.2:

$$A_1 = \pi(R_1 - t_1)^2 - \pi(R_1)^2 \quad (3.1)$$

$$A_2 = \pi(R_2 - t_2)^2 \quad (3.2)$$

$$A_3 = (H_1 - 2t_1)(W_1 - 2t_1) - (W_2)(H_2) = A_1 \quad (3.3)$$

$$A_4 = (H_2 - 2t_2)(W_2 - 2t_2) = A_2 \quad (3.4)$$

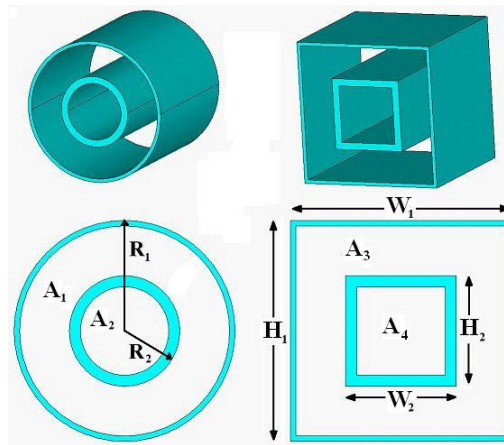


Figure 3.2 Equivalent square duct

By substituting Equations 3.1-3.2 into Equations 3.3-3.4 and assuming the $H_1 = W_1$ and $H_2 = W_2$, the dimensions for the square duct can be found.

3.1.3 Increasing the Wall Thickness

As stated before, this is a very thin bodied model and thus it required a large number of elements to mesh it. In order to try and reduce this number of elements, simulations were performed to determine if there is a correlation between a material's thickness and the way it behaves during thermal loading. To be more specific, the simulations were intended to determine if a material's properties can be scaled in way that would allow a similar thermal response of a model while having wall thicknesses that are larger than the fireplace's actual values. This would mean that the model could be designed with an increased thickness,

lowering the number of elements required to mesh the model, while still providing an accurate representation of how the fireplace would respond during thermal loading.

When performing a thermal simulation in ANSYS, the solution of temperature is uncoupled from pressure and velocity. This means that the equation of energy is the only system of equations used to solve for the temperature values throughout the model. For an incompressible analysis, the equation of energy can be written as(6);

$$\begin{aligned} \frac{\partial}{\partial t}(\rho C_p T) + \frac{\partial}{\partial x}(\rho v_x C_p T) + \frac{\partial}{\partial y}(\rho v_y C_p T) + \frac{\partial}{\partial z}(\rho v_z C_p T) \\ = \frac{\partial}{\partial x}\left(K_{xx} \frac{\partial T}{\partial x}\right) + \frac{\partial}{\partial y}\left(K_{yy} \frac{\partial T}{\partial y}\right) + \frac{\partial}{\partial z}\left(K_{zz} \frac{\partial T}{\partial z}\right) + Q_V \end{aligned} \quad (3.5)$$

where: ρ = Density

C_p = Specific heat

$v_{x,y,z}$ = Velocity in x,y,z directions

T = Temperature

$K_{xx,yy,zz}$ = Thermal conductivity in x,y,z directions

Q_V = Volumetric heat source

The velocities inside of the solid regions of the model will be zero because there is no fluid motion. Q_V will also be zero because there has been no heat source defined on the solid volumes. Also, the values of K_{xx} , K_{yy} , and K_{zz} are assumed to be constant. Making these simplifications to Equation 3.5 provides;

$$\frac{\partial}{\partial t}(\rho C_p T) = K_{xx} \frac{\partial^2 T}{\partial x^2} + K_{yy} \frac{\partial^2 T}{\partial y^2} + K_{zz} \frac{\partial^2 T}{\partial z^2} \quad (3.6)$$

Equation 3.6 can be integrated over a differential volume and will yield the following equation:

$$\int \int \int_{V_{ol}} \left(\frac{\partial}{\partial t}(\rho C_p T) \right) dx dy dz = \int \int \int_{V_{ol}} \left(K_{xx} \frac{\partial^2 T}{\partial x^2} + K_{yy} \frac{\partial^2 T}{\partial y^2} + K_{zz} \frac{\partial^2 T}{\partial z^2} \right) dx dy dz \quad (3.7)$$

If the thickness of the differential volume were to double in the x-direction, then Equation 3.7 would become:

$$\begin{aligned}
& \int \int \int_{Vol} \left(\frac{\partial}{\partial t} (\rho C_p T) \right) 2 dx dy dz \\
= & \int \int \int_{Vol} \left(K_{xx} \frac{\partial^2 T}{\partial (2x)^2} + K_{yy} \frac{\partial^2 T}{\partial y^2} + K_{zz} \frac{\partial^2 T}{\partial z^2} \right) 2 dx dy dz
\end{aligned} \tag{3.8}$$

After some manipulation, Equation 3.8 will become:

$$\begin{aligned}
& \int \int \int_{Vol} 2 C_p \left(\frac{\partial}{\partial t} (\rho T) \right) dx dy dz \\
= & \int \int \int_{Vol} \left(\frac{K_{xx}}{2} \frac{\partial^2 T}{\partial (x)^2} + 2 K_{yy} \frac{\partial^2 T}{\partial y^2} + 2 K_{zz} \frac{\partial^2 T}{\partial z^2} \right) dx dy dz
\end{aligned} \tag{3.9}$$

Equation 3.9 is the final form of the energy equation for a differential volume having a thickness in the x-direction equal to twice the original thickness. In order for this larger volume to have the same reaction under thermal loading as the original volume, Equation 3.9 and Equation 3.7 must be made equal. To do this, the values of K_{xx} , K_{yy} , K_{zz} , and C_p in Equation 3.9 can be scaled. Setting these parameters to the inverse of their coefficients will result in Equation 3.7 and Equation 3.9 being identical and thus, we have determined a way to model a solid with increased thickness that will perform the same during thermal loading as it would have with the original thickness. Using this method of scaling thermal properties allows the walls of the fireplace to be modeled with increased thickness, decreasing the amount of elements required to mesh the entire model. Verification of this method will be shown later in the analysis section of this document.

3.2 Design in ANSYS

Dimensions for the fireplace were taken directly from the ProE drawings provided by the manufacturer. Within the ProE software, there is a tool which allows the user to specify two points of a model and find the corresponding length between them. In this manner, the various distances making up the components of the fireplace were collected and solid models were then created in ANSYS using these values. The converted ProE model in ANSYS is shown below:

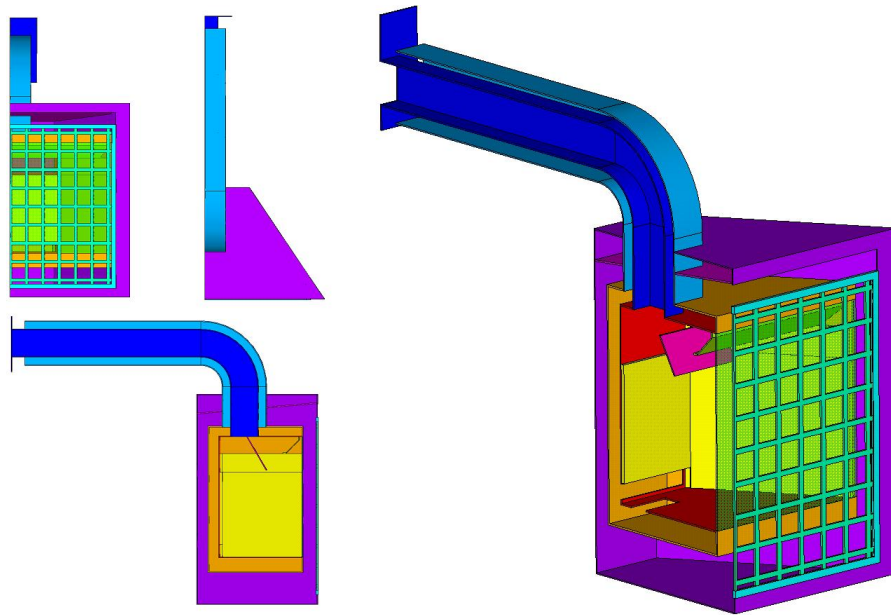


Figure 3.3 Fireplace model in ANSYS

3.3 Choosing Element Type

The ANSYS element type chosen for this research was Fluid141, an isoperimetric element with velocity, pressure, and temperature as its degrees of freedom. This element can be used to model transient or steady state fluid/thermal systems and allows the user to model both fluids and solids using one element type. While there are many element types available in ANSYS that deal with thermal analysis, Fluid141 is the only element that deals with thermal analysis as well as fluid flow in a 2-D solid, making it the ideal choice for this research. When using this element, the conservation equations for viscous fluid flow and energy are solved in the fluid region, while only the energy equation is solved in the non-fluid region. For the FLOTRAN CFD elements, the velocities are obtained from the conservation of momentum principle, the pressure is obtained from the conservation of mass principle, and the temperature is obtained from the law of conservation of energy. A segregated sequential solver algorithm is used; that is, the matrix system derived from the finite element discretization of the governing equation for each degree of freedom is solved separately. The flow problem is nonlinear and the governing equations are coupled together. The sequential solution of all the governing

equations, combined with the update of any temperature- or pressure-dependent properties, constitutes a global iteration. The number of global iterations required to achieve a converged solution may vary considerably, depending on the size and stability of the problem.

3.4 Materials

3.4.1 Aluminized Steel and Galvanized Steel

The majority of the fireplace structure is made up of two types of steel; galvanized steel and aluminized steel. The galvanized steel has a fine outer coating of zinc whereas the aluminized steel has a coating of aluminum. The overall thicknesses of the steels range from 0.021” to 0.028” with about 0.0015” of that thickness being the coatings of zinc and aluminum. This results in a ratio of steel to coating of approximately 14:1. The steel used is a low-carbon steel with a carbon content of 0.05-0.15% by weight. The steel used in this fireplace is provided by AK Steel. The thermal properties for these two steels can be found on their website and are listed in Table 3.1.

3.4.2 Fiber Refractory

Fiber refractory is a material used for insulation inside of the fireplace. It is placed on the surface of the steel walls located inside of the combustion chamber of the fireplace. It is designed to be stable at very high temperatures and can be engineered to have the desired thermal properties for specific applications. For use in fireplace applications, a fiber refractory must have low values of thermal conductivity and high specific heat. This will reduce the amount of heat that is passed through the refractory and into the surrounding steel walls. The thermal properties for the refractory were provided by the fireplace manufacturer and are listed in Table 3.1.

3.4.3 Tempered Glass

Tempered glass is glass that has been processed by controlled thermal or chemical treatments to increase its strength compared with normal glass. Along with increased strength comes an increased resistance to heat transfer which allows the glass to be used as another means of thermal insulation. In the fireplace, this glass is located on the forward facing wall of the combustion chamber. This allows the operator to see the flame while also providing thermal insulation. The values for the tempered glass used in this model of fireplace were provided by the fireplace manufacturer and its thermal properties are listed in Table 3.1.

Table 3.1 Thermal properties of aluminized and galvanized steel

Material	Density, ρ ($\frac{lb_f s^2}{in^4}$)	Conductivity, K ($\frac{BTU}{in-\circ F-sec}$)	Specific Heat, C_p ($\frac{BTU}{slug-\circ F}$)
Aluminized Steel	7.3E-4	6.94E-4	50.19
Galvanized Steel	7.2E-4	1.19E-3	45.28
Fiber Refractory	2.4E-5	1.54E-6	96.52
Tempered Glass	2.3E-4	1.27E-5	73.36
Aluminum Screen	2.54E-4	3.15E-3	92.66

3.4.4 Air

The thermal properties for air are catalogued within ANSYS and can be accessed when performing CFD analysis using FLOTTRAN. These values are able to vary with temperature and also allow for variable air density. The proper unit system must be chosen when selecting the thermal properties of air and should match those used to dimension the model as well as the units of any boundary conditions or initial conditions placed on the system.

The model of this fireplace uses the idea of a natural convection or buoyancy driven flow. In this setup, the flow of air is brought about due to the changing density of air as the temperature rises. This change in density is calculated within ANSYS at each global iteration and is done using the following equation:

$$\rho = NOMI * \left(\frac{P}{COF_2}\right) / \left(\frac{T}{COF_1}\right) \quad (3.10)$$

where: NOMI = Nominal density at sea level conditions

COF_1 = Value of temperature when $\rho=NOMI$

COF_2 = Value of pressure when $\rho=NOMI$

T = Nodal temperature

P = Nodal pressure

It is easily verified that when pressure and temperature are at their nominal values then the solution to Equation 3.10 is NOMI, the nominal value of density.

ANSYS also provides air properties specifically for use with buoyancy driven flows. When this option is selected, the value for pressure in Equation 3.10 is set to the nominal value COF_2 each time the variable density is calculated. This reduces density to a function of temperature only as is the case in most buoyancy driven flows.

CHAPTER 4. Results

4.1 Thickness Study

In Section 3.1.3, manipulation of the energy equation determined that it is possible to obtain identical solutions for a thermal simulation of two materials of different thicknesses by scaling the thermal properties of one of the materials. In the following section, the results of a simple FLOTRAN analysis are presented to verify this formulation.

Figure 4.1 illustrates the setup for this analysis. Three solid walls with varying thickness were subjected to an identical heated flow. Referring back to Section 3.1.3, in order for these three walls to behave similarly under thermal loading, Equation 3.7 and Equation 3.9 must be made equal to each other. This is done by multiplying the value K_{xx} , K_{yy} , K_{zz} , and C_p by the inverse value of their coefficients. For the case of double thickness, as is the case in the equation formulation, K_{xx} must be multiplied by a factor of two and K_{yy} , K_{zz} , C_p must be halved. With these changes made to Equation 3.9, it will now be identical to Equation 3.7. Similar thermal property scaling must be done for the triple thickness wall as well.

The wall were modeled as aluminum with the following thermal properties(5):

Table 4.1 Thermal properties of aluminum walls of varying thickness

Thickness	ρ ($\frac{kg}{m^3}$)	K_{xx} ($\frac{W}{m^{\circ}C}$)	K_{yy} ($\frac{W}{m^{\circ}C}$)	K_{zz} ($\frac{W}{m^{\circ}C}$)	C_p ($\frac{J}{kg^{\circ}C}$)
t	2800	143	143	143	795
2t	2800	246	71.5	71.5	397.5
3t	2800	429	47.7	47.7	265

The values used for air were those stored in ANSYS for the SI unit system and are listed below. For this simulation the air was not allowed to have variable density and thus the values

for COF_1 and COF_2 have been omitted.

Table 4.2 Thermal properties of air

ρ ($\frac{kg}{m^3}$)	K ($\frac{W}{m^{\circ}C}$)	C_p ($\frac{J}{kg-^{\circ}C}$)
1.205	2.5743E-2	1.0040E3

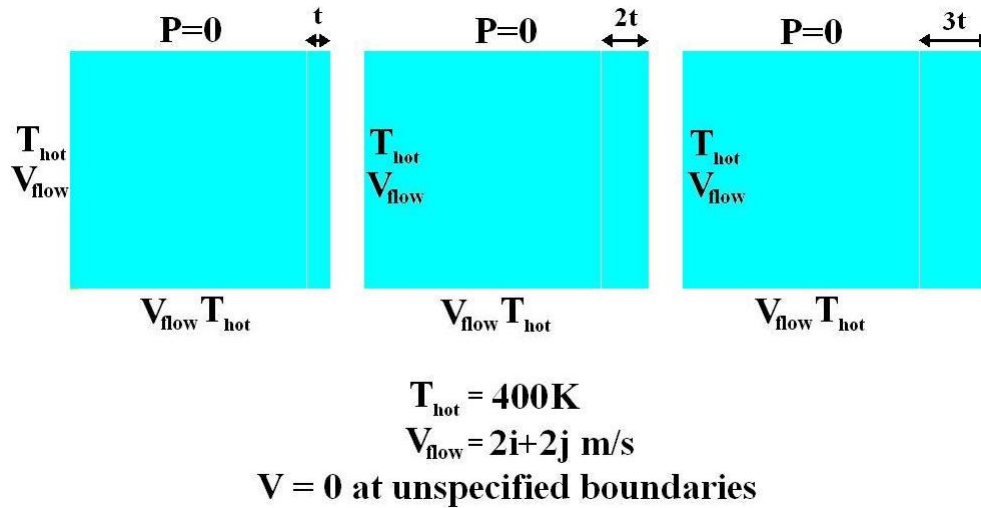


Figure 4.1 Setup for thickness analysis

After supplying ANSYS with the thermal properties for each constituent, the model was then meshed. Meshing was done by setting the element spacing on each line of the model. By meshing in this manner, it is ensured that the nodes in each solid section will be in the same place with respect to their thickness. This makes comparing the nodal solutions of each solid area a very easy task. The meshing scheme used for this model is shown in Figure 4.2. Here each line has been set to have thirty total elements resulting in thirty-one nodes on each line.

After meshing the model, a transient analysis was performed over a period of 1000 seconds, allowing the walls to heat up. Figures 4.2 - 4.4 show the final solutions for temperature on the wall, and velocity and pressure respectively. The solutions for velocity and pressure are identical for each model and only the solution from original thickness simulation is shown. In Figure 4.5, the time rate of change of temperature is shown for the same location on each of the three walls. Also, the temperature distribution along the horizontal centerline of each wall

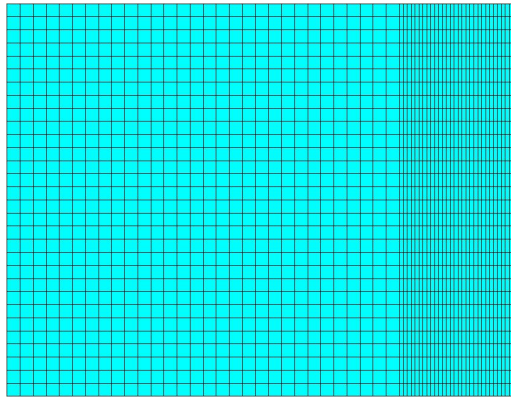


Figure 4.2 Meshing with 30 elements/line

at Time = 1000 sec is shown in Table 4.1. When looking at the results shown in Figure 4.5 and Table 4.1, we can now see that indeed the solutions are identical as was proven mathematically in Section 3.1.3. In Figure 4.5, the lines are perfectly overlapped and thus only one of the lines appears. This means that the thickness for the fireplace can be increased while still allowing for an accurate representation of the fireplace's thermal response.

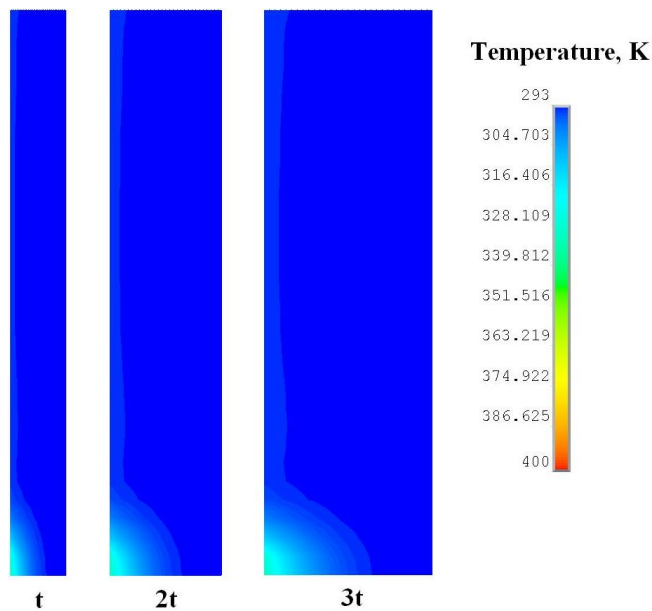


Figure 4.3 Temperature contour for each solid area

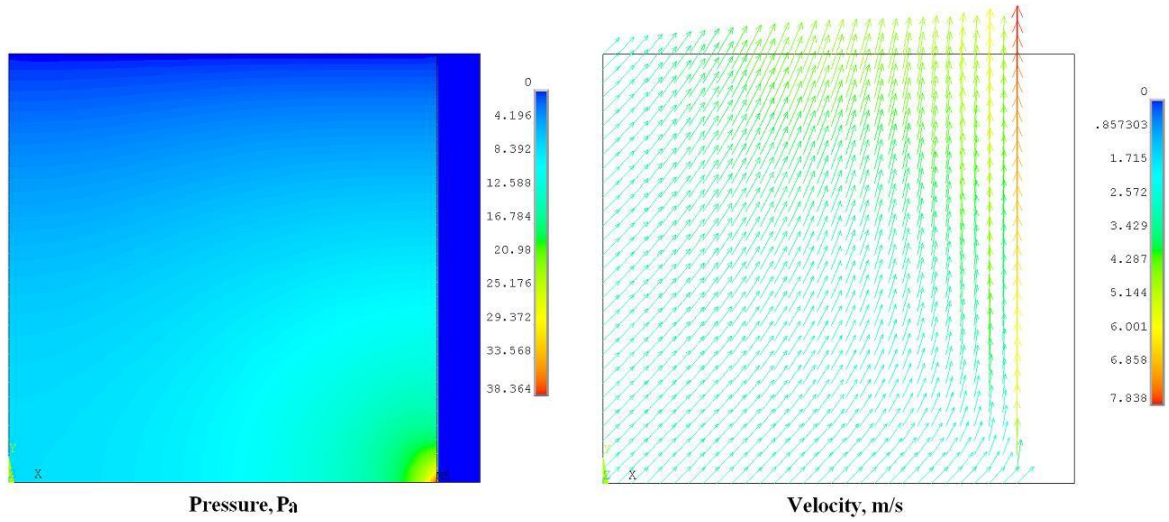


Figure 4.4 Pressure and velocity vector contours

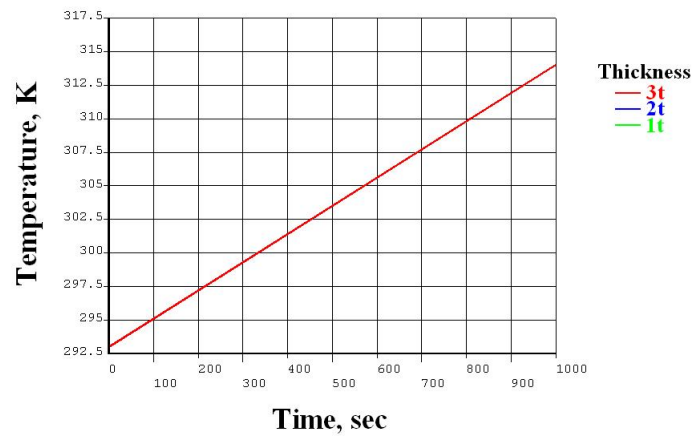


Figure 4.5 Temperature over time for varying wall thickness

Table 4.3 Temperature along the horizontal centerline

1t		2t		3t	
x-location (m)	Temp (K)	x-location (m)	Temp (K)	X-location (m)	Temp (K)
0.0	294.12	0.0	294.12	0.0	294.12
0.1	293.72	0.2	293.72	0.3	293.72
0.2	293.44	0.4	293.44	0.6	293.44
0.3	293.25	0.6	293.25	0.9	293.25
0.4	293.13	0.8	293.13	1.2	293.13
0.5	293.06	1.0	293.06	1.5	293.06
0.6	293.03	1.2	293.03	1.8	293.03
0.7	293.01	1.4	293.01	2.1	293.01
0.8	293.00	1.6	293.00	2.4	293.00
0.9	293.00	1.8	293.00	2.7	293.00
1.0	293.00	2.0	293.00	3.0	293.00

4.2 Example 1

Before modeling the actual fireplace in ANSYS, a simpler model was created. This model was designed to have many of the same features of the actual fireplace, while eliminating some of the more complicated geometries such as the flue and glass shields which greatly alter the flow through the inner chamber. The model was also designed with an increase thickness, however the thermal properties have been scaled in order to simulate how the walls of the fireplace will react under thermal loads. This simulation was performed to test out the boundary conditions that would eventually be applied to the fireplace as well as locate any areas that may cause problems when solving 2-D flow. The setup for this analysis is depicted in Figure 4.6. The air flow for this simulation is a mixed flow, meaning it is driven by both forced convection as well as natural convection. At the inlet, a velocity of $25 \frac{in}{sec}$ in the x-direction is applied with no component of velocity allowed in the y-direction. All other walls have been given a no-slip condition, meaning the flow stays attached to the wall and consequently has a velocity of zero. At the outlet, a zero relative pressure condition is set and the temperature is at a constant 400°F. This is an arbitrary value set in order to allow for a heat flux across the surface. In ANSYS, if a thermal boundary condition is not prescribed on an external wall then it is assumed that the heat flux across that boundary is zero and the flow at the boundary would

eventually reach that of the heat source. Before running the simulation, the Reynolds number (Re) for the flow had to be determined. This is a dimensionless property which describes the ratio of inertial forces to viscous forces (4). Flow through a duct is generally considered a laminar flow if $Re < 2300$ and a turbulent flow for $Re > 4000$. Between the two ranges, the flow can be shown to exhibit characteristics of both laminar and turbulent flow. The equation for Reynolds number for a rectangular duct is given below, along with the subsequent calculation for this model. Here a unit distance has been assumed for the off-axis length:

$$Re = \frac{\rho V D_h}{\mu} = \frac{1.1172E - 7 * 25 * 1.5}{2.6497E - 09} = 1581.12 < 4000 \quad (4.1)$$

where: D_H = Hydraulic diameter = $\frac{2LW}{L+W}$

L=Length

W=Width

Equation 4.1 shows that the Reynolds for this outlet is below that for turbulent flow and thus the model has been simulated in ANSYS as a laminar flow.

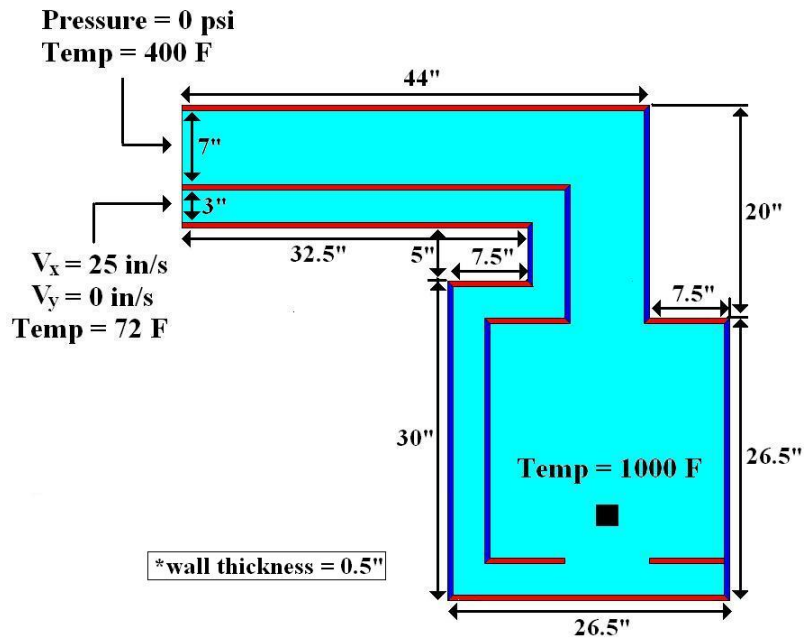


Figure 4.6 Setup for Example 1

As stated before, this model was designed with an increased thickness compared to the actual fireplace. The blue and red walls differentiate between those with an increased thickness in the x-direction and the y-direction, with the blue walls being in the x-direction and the red walls in the y-direction. As was shown in Section 2.3.1 there is a sort of orthogonality with the thermal property scaling. The proper value of thermal conductivity must be applied for each direction, with K_{xx} increasing for a thickness increase in the x-direction whereas for a thickness increase in the y-direction, K_{yy} must be increased. The thermal properties for both the wall and air are listed in Table 4.4. The units used for this model will result in pressure units in psi. For this analysis, the walls have been modeled as aluminized steel. The (x) and (y) in Table 4.4 designate a thickness increase in the x- or y-direction.

Table 4.4 Thermal properties for Example 1

Material	ρ ($\frac{\text{slug}}{\text{in}^3}$)	K_{xx} ($\frac{\text{lb-f-in}}{\text{in-}^\circ\text{F-sec}}$)	K_{yy} ($\frac{\text{lb-f-in}}{\text{in-}^\circ\text{F-sec}}$)	K_{zz} ($\frac{\text{lb-f-in}}{\text{in-}^\circ\text{F-sec}}$)	C_p ($\frac{\text{lb-f-in}}{\text{slug-}^\circ\text{F}}$)
Alum. Steel (x)	7.3E-4	6.94E-3	6.94E-5	6.94E-5	5.19
Alum. Steel (y)	7.3E-4	6.94E-5	6.94E-3	6.94E-5	5.19
Air	1.1172E-07	3.4683E-07	””	””	9.2650E+01

4.2.1 Example 1 Results

A steady state simulation was performed for this model with the boundary conditions shown in Figure 4.6. The results for that model are shown in Figures 4.7-4.10.

The most notable results for this simulation can be seen in Figures 4.7 and 4.10. Here, the temperature contour, velocity contour and velocity vector plots are illustrated. These plots reveal that the zero relative pressure condition which was enforced on the outlet is not a sufficient boundary condition for this flow. In general forced convection flow, this condition is perfectly acceptable given the outlet is located far enough downstream and the flow has reached a steady state. However, in this model both forced and natural convection flow are used and while we can see that the flow has indeed reached a steady state, the temperature and pressure are not constant along this flow due to the fact that the air density is changing. This means that it is impossible to satisfy the constant temperature and constant pressure conditions at

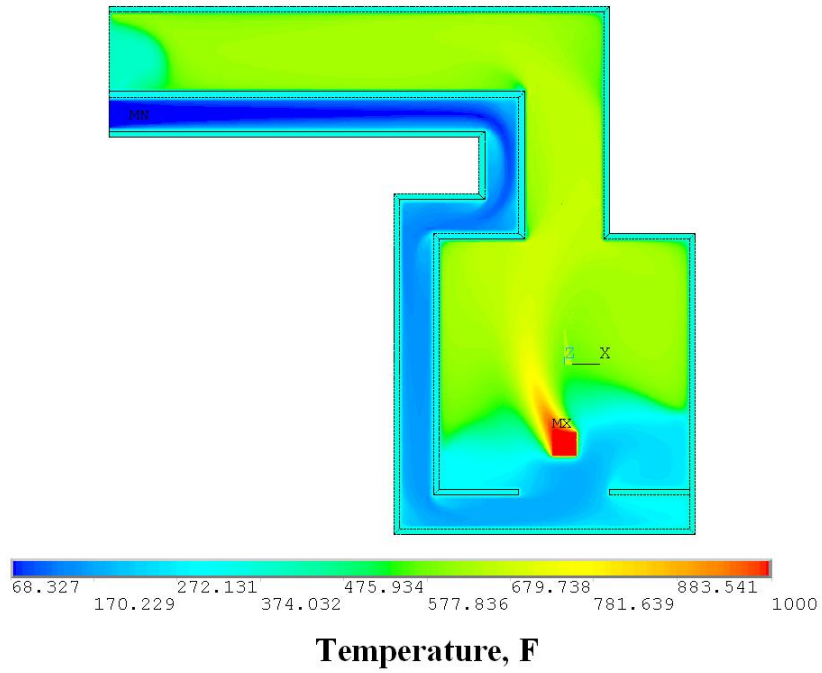


Figure 4.7 Example 1 temperature contour plot

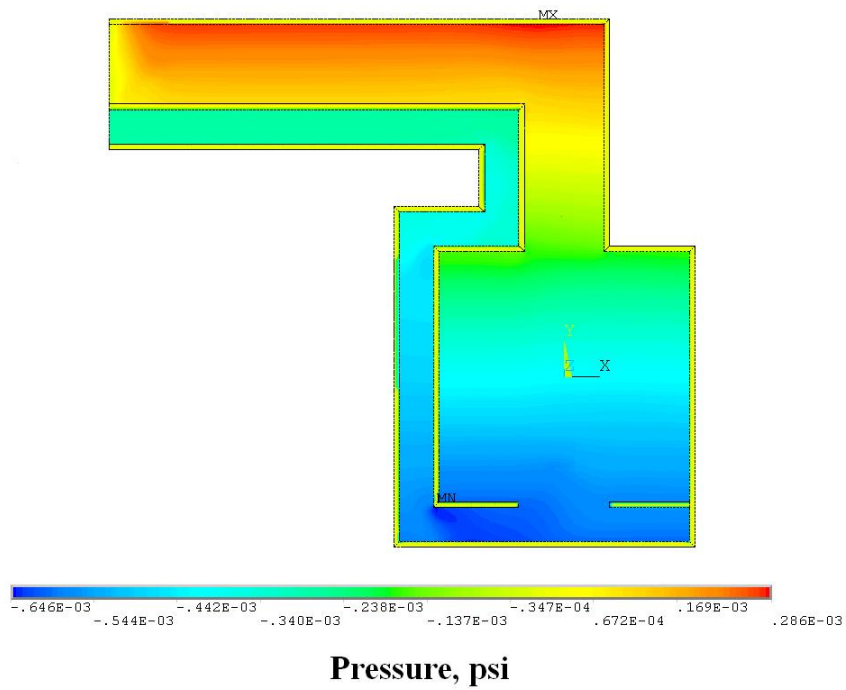


Figure 4.8 Example 1 pressure contour plot

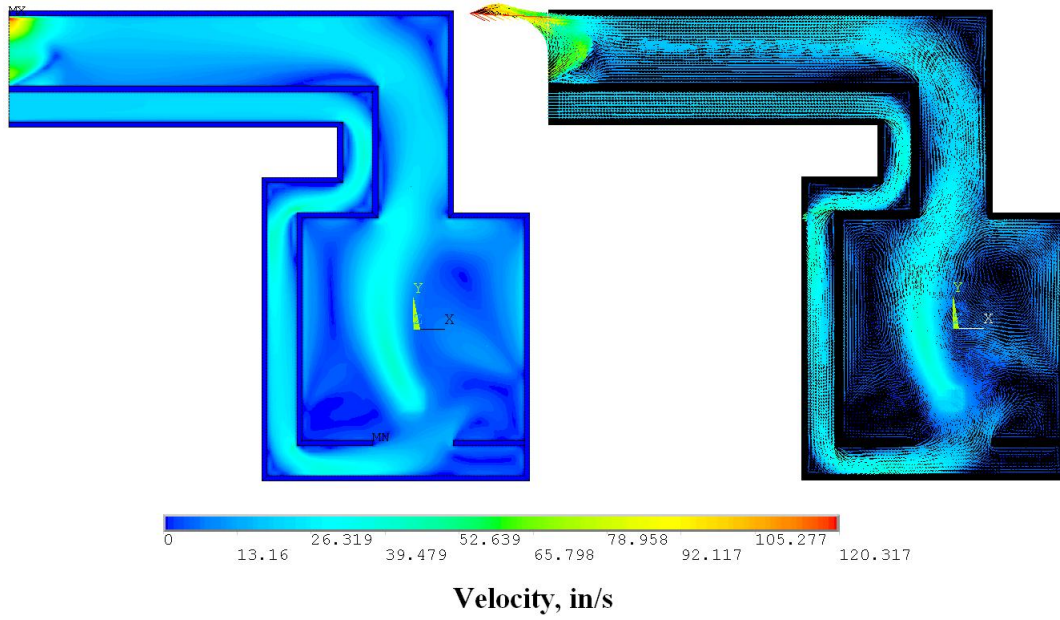


Figure 4.9 Example 1 velocity contour and vector plots

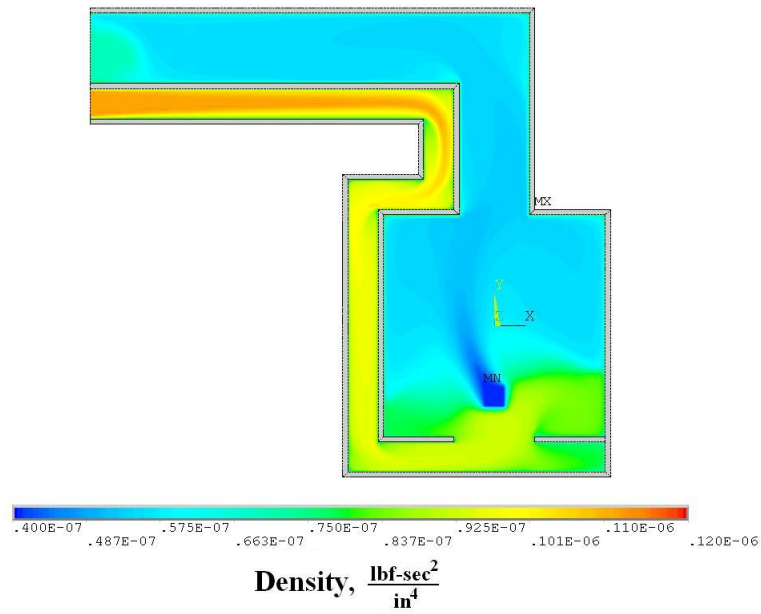


Figure 4.10 Example 1 density contour plot

the outlet unless the velocity is allowed to change significantly. Figure 4.11 provides a good illustration of what is exactly happening at the outlet. As the hotter air in the upper portion of the flow reaches the outlet, the temperature and pressure conditions placed on the outlet force the temperature and pressure of the flow to decrease in order to match that boundary condition. This pressure difference causes flow to increase in the direction of lower pressure. This increase in velocity causes a vortical flow with the lower air rotating upwards to fill in where the air has vacated. This is obviously not the desirable effect at the outlet and thus a better set of boundary conditions is needed to be used in order model the flow at the outlet of the duct.

It would be possible for an experimentalist to take the measurements for both pressure and temperature at the outlet and then apply them to the Finite Element model accordingly, however the idea of using the Finite Element model is to reduce the design phase of production and this would simply add more measurements needing to be taken. Also, the conditions at both the inlet and outlet will rarely be identical, and thus applying these boundary conditions would only accurately model this one case and would not allow the variation of things such as geometry, heat added into the system, as well as different ambient conditions under which the unit may operate. The decision was made instead to model the fireplace in a room with the exhaust exiting to a large open source of air at atmospheric conditions. This provides a closer approximation to the actual conditions the fireplace will operate under. The subsequent models have been simulated in this manner.

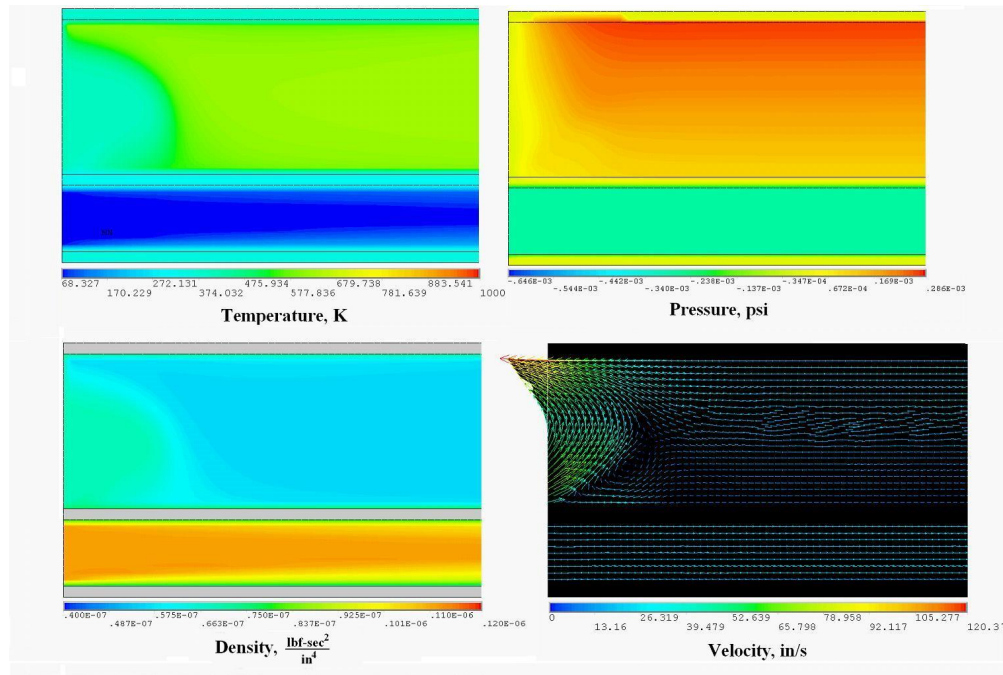


Figure 4.11 Conditions at the outlet

4.3 Example 2

The following model was created using the existing model presented Section 3.2, however, for this simulation the ambient outside air has been added in order to eliminate the need to specify the boundaries at the inlet and outlet. This allows for a more dynamic model that can be run under many different conditions with varying inputs. The idea is to be able to simulate a multitude of changes within the system itself such as, different heat sources (propane or natural gas for instance), different geometries of the fireplace (different venting and duct geometry), as well as different ambient conditions. For instance, the value of ρ plays a very large roll in natural convection and can be shown to change significantly as elevation is increased as well as ambient temperature and pressure conditions. All of these values can be taken into account using the current model as they are all inputs into the system. The setup for this simulation is illustrated in Figure 4.12. The dimensions for this model are the same as those in Example 1, and the two areas representing the room air and ambient room air are both 120" x 120".

Here, the boundaries having no-slip conditions enforced on them are considered to be the

walls of the room in which the fireplace is located. These walls are modeled as being perfectly insulated with no heat loss through them. While this is not a perfect boundary condition to be imposed, it is difficult to estimate how much heat is lost through a wall. This number is highly dependent on the structure of the wall as well as other conditions such as the number of windows and doors located in the room, the R-value of the insulation being used, and even the number of outlets and ceiling fans (8). These will all play a role in determining the heat lost from a room and thus a simpler condition of zero heat loss has been used. The boundary between the outside ambient air and the air of the room has also been separated by a perfectly insulated wall with a no-slip condition imposed on it. The actual wall itself need not be modeled as the no-slip boundary condition will restrict any flow from crossing through it. There is also small area located behind the fireplace, between it and the outside air, which has been neglected. The air entering the inlet duct of the fireplace will be at room temperature and thus the backside wall of the fireplace should remain at a temperature close to the ambient temperature of 72°F.

The thermal properties used for this simulation are the same as those used before in Example 1, listed in Table 4.4. For this model, only natural convection was used as the driving force for fluid flow. As the air around the heat source expands due to the temperature increase, the density will decrease as per Equation 2.10. This will cause a pressure loss as the air vacates that area and the air located in the inlet will then flow towards that area of lower pressure and thus a flow will begin.

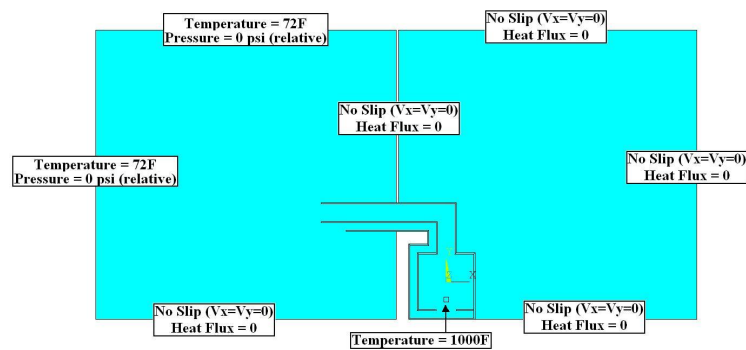


Figure 4.12 Setup for Example 2

4.3.1 Example 2 Results

A transient analysis was performed on this model over the course of 200 seconds using the boundary conditions shown in Figure 4.12. The results of that simulation are given below. Figures 4.13-4.16 provide illustrations of the solutions for temperature, pressure, velocity and density. When looking Figure 4.14, we can now see that the zero relative pressure boundary conditions imposed on the outlet in Example 1 was indeed an incorrect condition. The pressure is seen to range from 0 psi to 0.138E3 psi from the bottom of the outlet to the top. Again, this is due to the buoyancy forces at the outlet which force the hotter, less dense air, to rise creating an increased pressure in the upper portion of the duct. Also, looking at Figure 4.13, the constant temperature boundary condition which was set on the outlet in the previous example appears to be a correct assumption. However, directly at the outlet we can see that this condition is also unsatisfactory. Again, the warm air rises as it meets the cooler ambient air and thus the temperatures seen at the outlet increase from the bottom to the top. It is worth noting that from looking at these solutions, it would seem that a vertically vented fireplace could be modeled with conditions similar to those in Example 1 with a fair amount of accuracy. Here the buoyancy forces would be acting in the direction of the airflow and, assuming a constant temperature across the outlet, the density would remain constant at the outlet as well as the pressure and velocity.

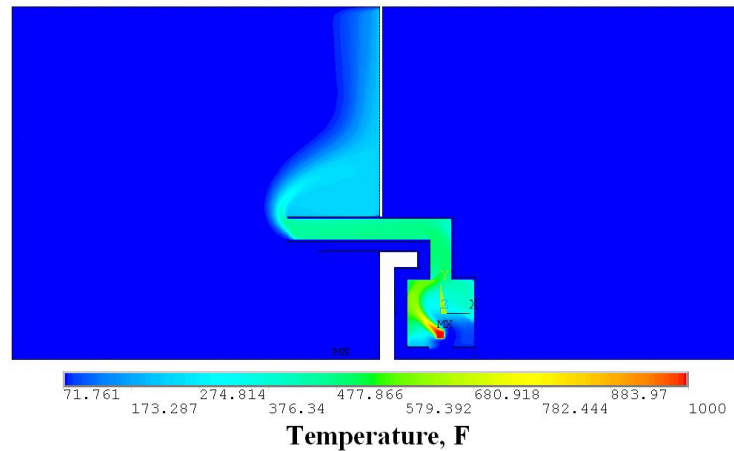


Figure 4.13 Temperature contour for Example 2

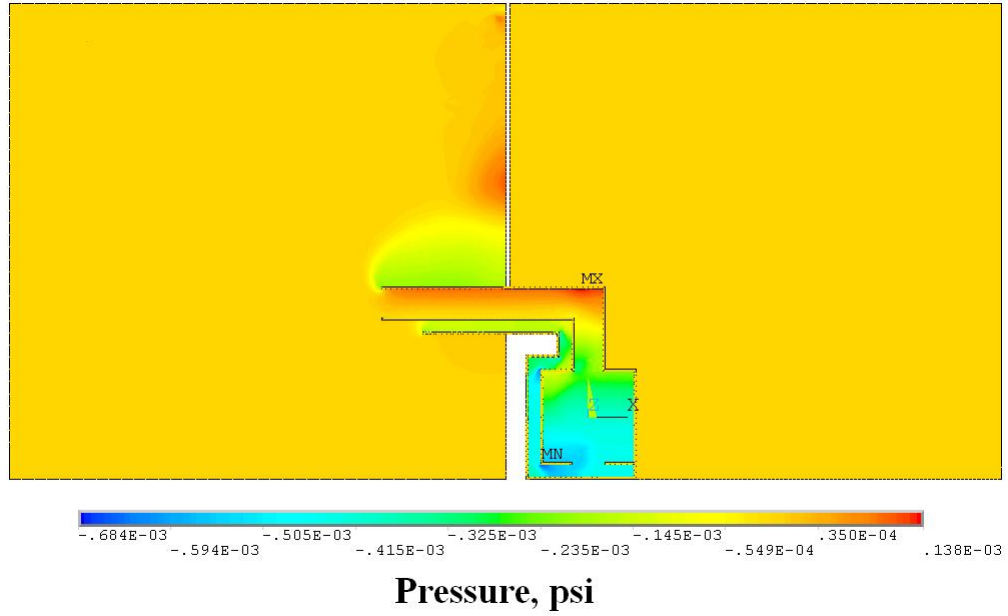


Figure 4.14 Pressure contour for Example 2

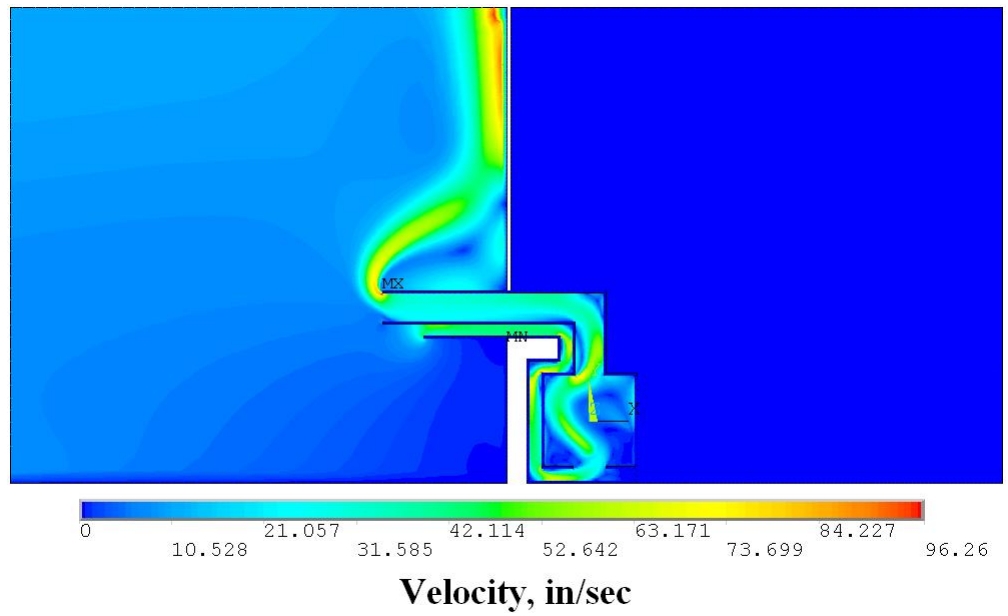


Figure 4.15 Velocity contour for Example 2

Figures 4.17-4.19 provide a closer look at the solutions inside of the example fireplace. From looking at the temperature distribution shown in Figure 4.17, it seems that the period of 200 seconds has not been long enough to allow enough heat through the walls in order to increase the temperature of the room outside of the fireplace. When modeling the actual fireplace, a longer transient solution will be performed in order to see the effects of the fireplace on the air inside of the room.

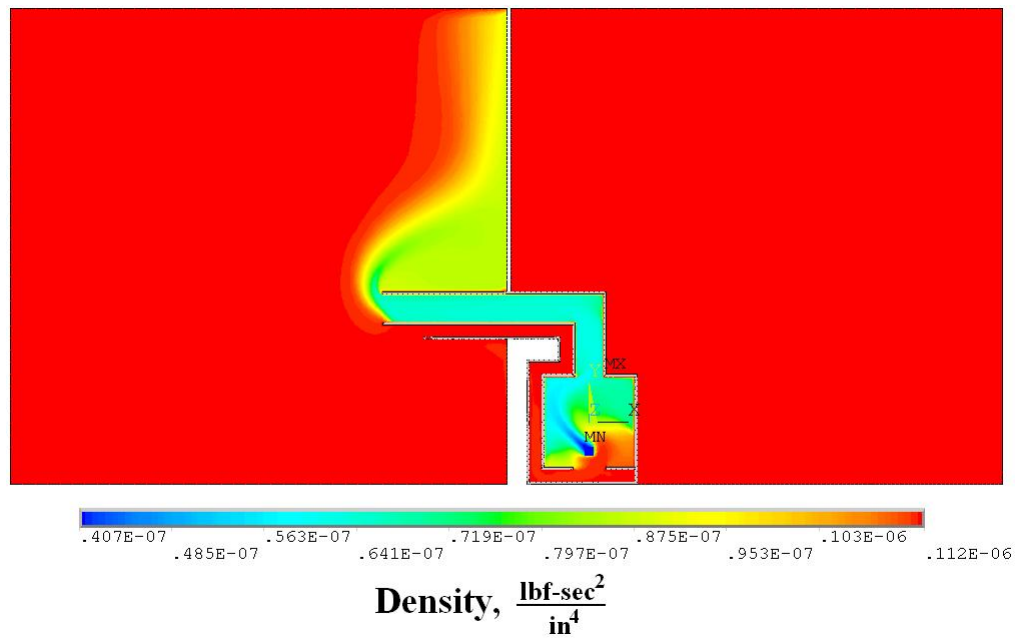


Figure 4.16 Density contour for Example 2

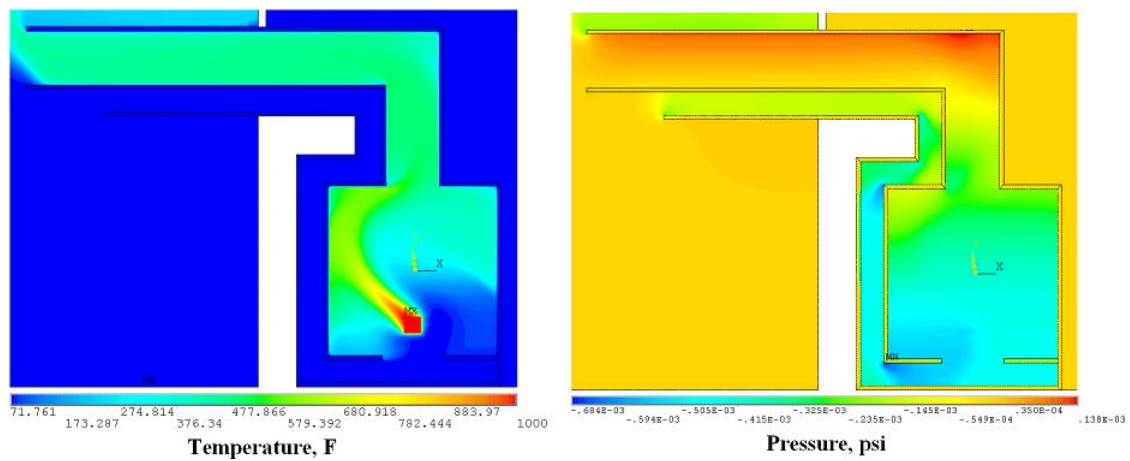


Figure 4.17 Temperature and pressure contour closeup for Example 2

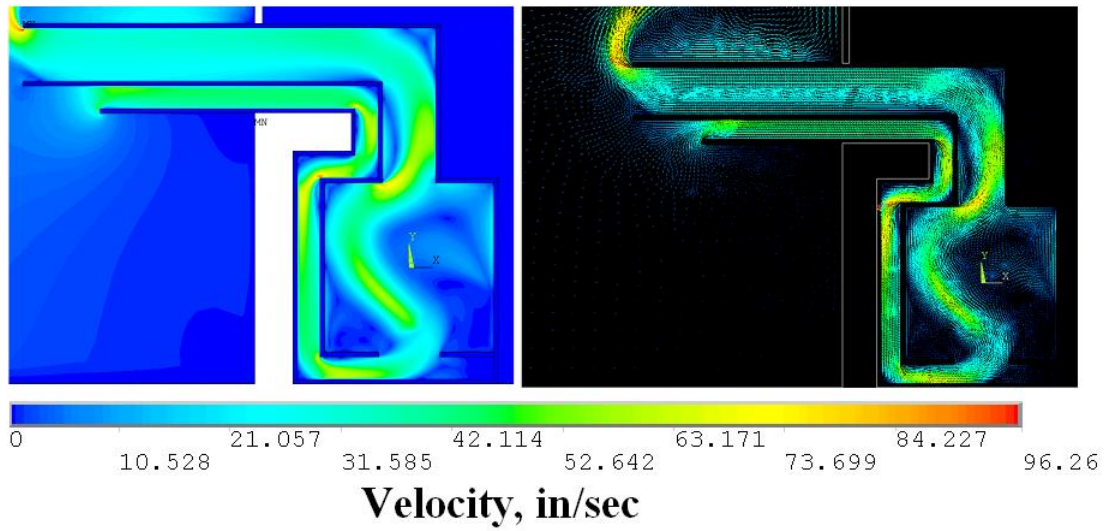


Figure 4.18 Velocity contour and vector closeup for Example 2

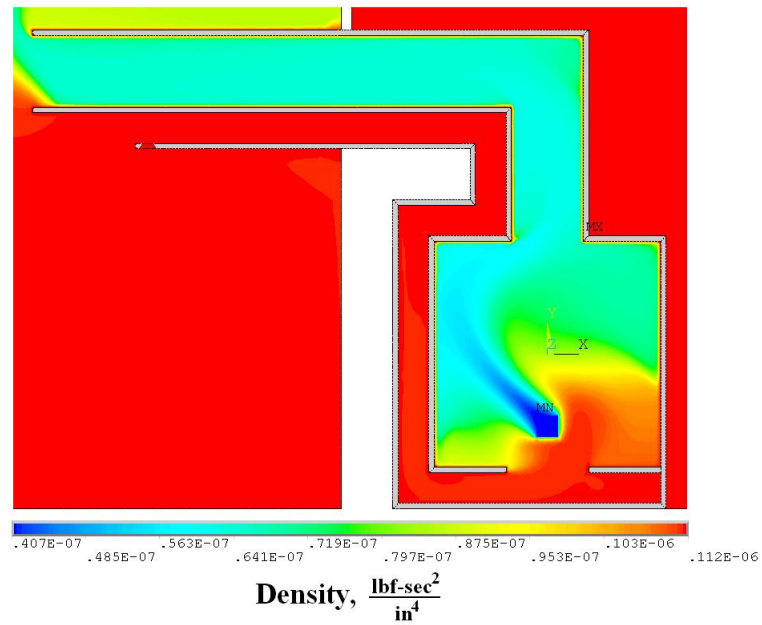


Figure 4.19 Density contour closeup for Example 2

4.4 2-dimensional Fireplace

In this section, the analysis of a 2-dimensional cross-section of the fireplace will be discussed along with the results of that analysis. To build this model, the cross-section of the original 3-dimensional fireplace was used. This was obtained by essentially cutting the model in half in ANSYS and then extracting the new surface created along that cut. An illustration of this process is shown below in Figure 4.20. This is not the complete model however. After extracting the cross-sectional area, the areas for both the outside and room air had to be created. For this model, the decision was made to increase the area of the outside air. Looking at the temperature contour for the previous analysis in Figure 4.13, the temperature at the upper boundary of the outside air was still around 200°F before the boundary condition at that point forced the flow to reach a temperature of 72°F. This is not a desirable result. In actuality, the temperature would steadily reach the ambient temperature of the outside air. It appears that the boundary conditions is still too close to the areas of interest in this model and has caused adverse effects on the solution. The final model for this simulation, along with the boundary conditions, is illustrated in Figure 4.21. The boundary conditions selected for this simulation were identical to those used in the Example 2 analysis.

Before continuing on to the analysis and results, there are some discrepancies between the 3-dimensional and 2-dimensional models that should be addressed first. As a result of

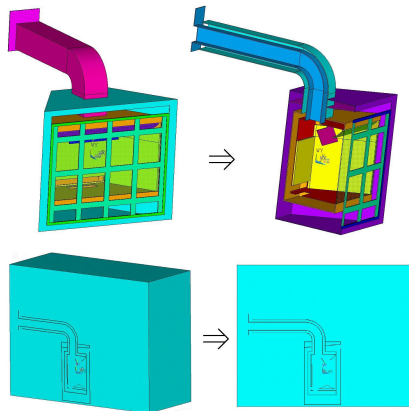


Figure 4.20 Obtaining the 2-dimensional cross-section

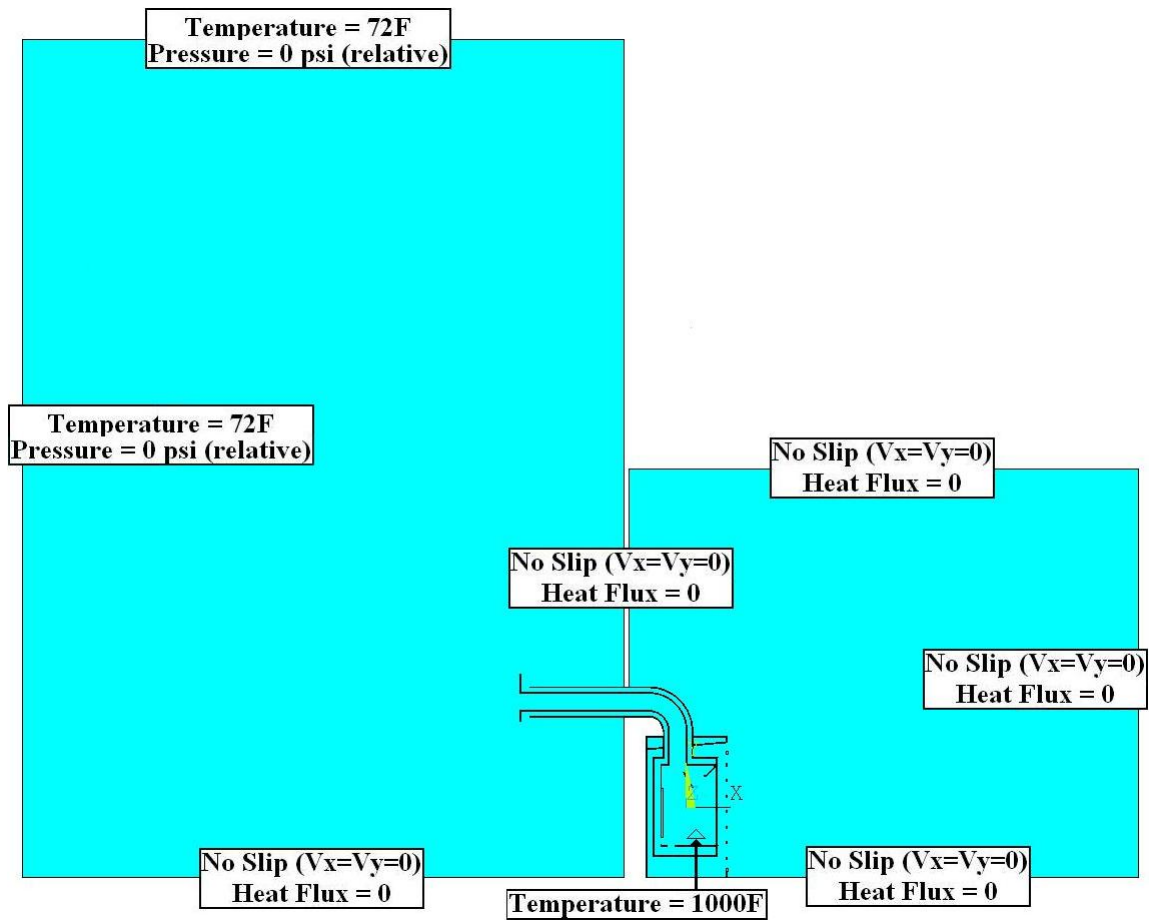


Figure 4.21 Setup for 2-d fireplace analysis

converting the original model into a 2-dimensional one, some of the paths in which air is supposed to pass freely have been blocked. One of these spots involves the upper portion of the outer duct through which ambient air flows into the fireplace for combustion. Figure 4.22 provides a closer inspection of this area with a comparison between the 3-dimensional and 2-dimensional model. The figure on the left depicts the flow as it should be in 3-dimensions. Here, air from the outside flows through the outer duct and makes its way to the backside of the fireplace and eventually the bottom where the internal combustion takes place. The 2-dimensional figure on the right does not allow this to happen. Here, the flow is obstructed by the inner duct wall and cannot pass through it, essentially eliminating any flow through the upper portion of the duct. It can be expected that the temperature of the air in the upper duct will be much higher than in reality as a result of this modeling discrepancy. There will no longer be a supply of cool air from the outside running through the outer duct and thus, as the hot air evacuating the fireplace passes through the inner duct, heat will be transferred to the air in the upper portion of the outer duct at a much faster rate due to the absence of convective cooling on the outer surface of this duct wall. It is likely that over the course of time enough heat will be allowed to pass into this region of air that even the air inside the room will see a higher temperature than normal.

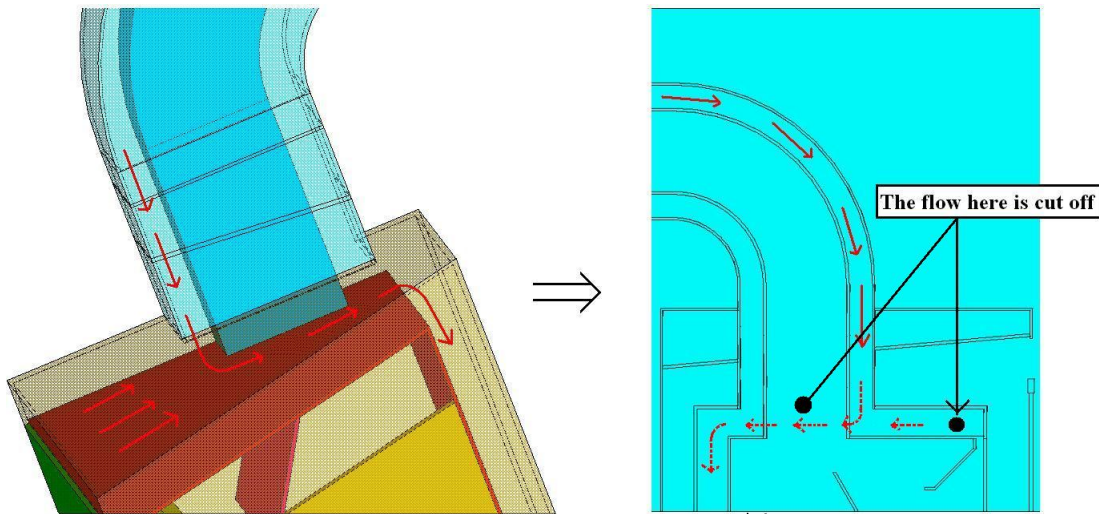


Figure 4.22 Poor inlet air flow model resulting from conversion to 2-dimensions

A similar effect can be seen when looking at the 2-dimensional view of the outer shell shown in Figure 4.22. Here, air from the room is supposed to be able to flow freely through the cavity between the inner and outer shells of the fireplace. This results from heat passing through the walls of the inner chamber of the fireplace and increasing the temperature of this air cavity. This causes the density of the air to decrease causing air to flow upwards through the cavity. This air flow then enters the room, supplying it with warm air. This is a common medium for heat transfer as it eliminates the need for a person to be directly in front of the fireplace in order to feel the heat from the fireplace. In this 2-dimensional model, the air flow is again blocked by the duct work at the top of the fireplace preventing this air flow into the room.

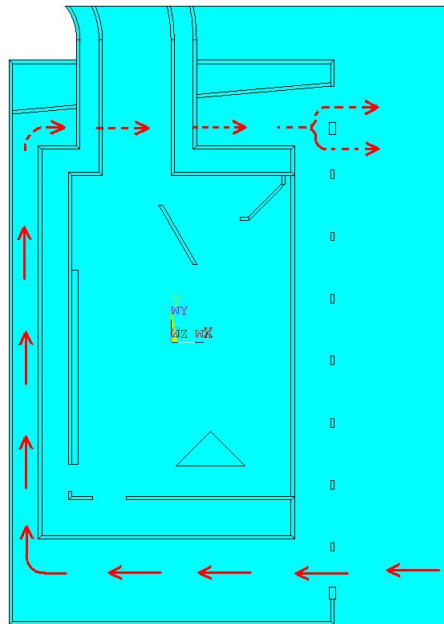


Figure 4.23 Incorrect air flow path resulting from conversion to 2-dimensions

4.5 Results

A transient analysis was performed for this model over the course one hour using the boundary conditions shown in Figure 4.21. The results of that analysis are provided in the following section. These results will then be compared to experimental data provided by the fireplace manufacturer which was also taken after the fireplace had been running for one hour.

The solutions for temperature, pressure and density for the system are illustrated in Figures 4.24-4.26.

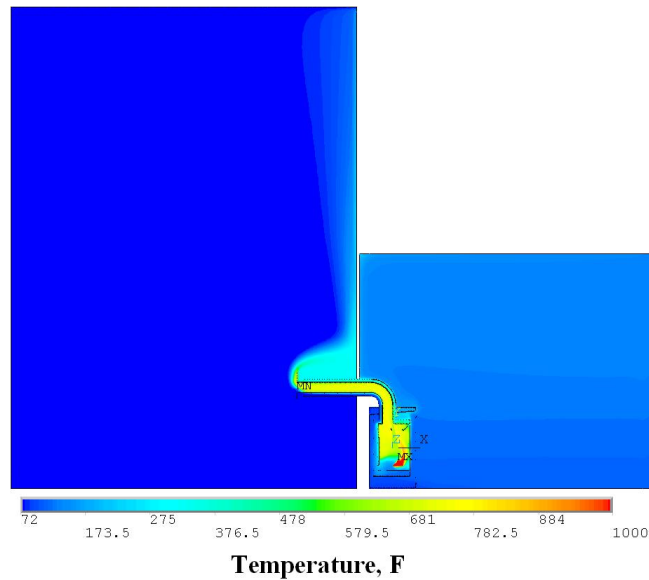


Figure 4.24 2-dimensional fireplace temperature contour plot

Looking at these contour plots, it appears that the system in this analysis performs very similarly to that in the Example 2 simulations. During this analysis however, the temperature has now been given ample time to pass through the walls of the inner chamber resulting in an increased temperature inside of the room. This was not the case for the previous analysis which was only run over a time period of 200 seconds. With this analysis, the pressure and density inside of the room can now be seen to fluctuate from the bottom of the room to the ceiling due to the heat transfer into the room. It is difficult to draw any other conclusions without first taking a closer look at the results inside the fireplace itself.

The focus for the remainder of this section will be on the temperature and velocities solutions for this simulation in and around the fireplace. There is little correlation that can be made for pressure and density at this point due to a lack of experimental results for comparison. The temperature values around the fireplace are available however and thus a comparison between the analytical solution and experimental solutions can be made. Figures 4.27-4.29 illustrate the results for this analysis inside of the fireplace.

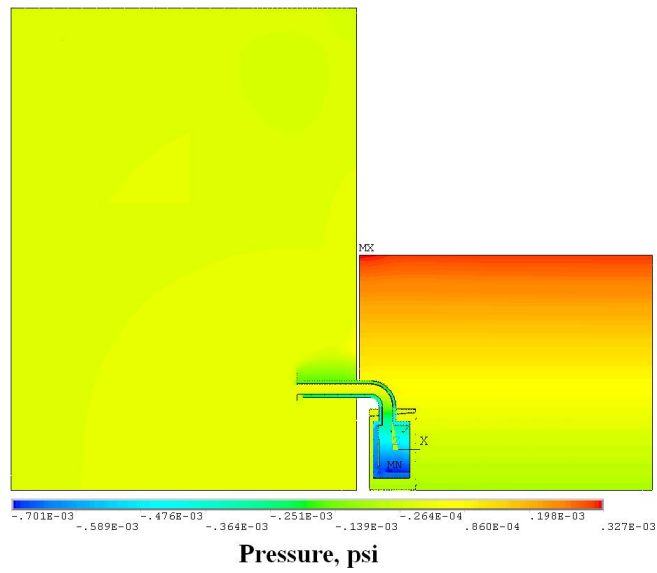


Figure 4.25 2-dimensional fireplace pressure contour plot

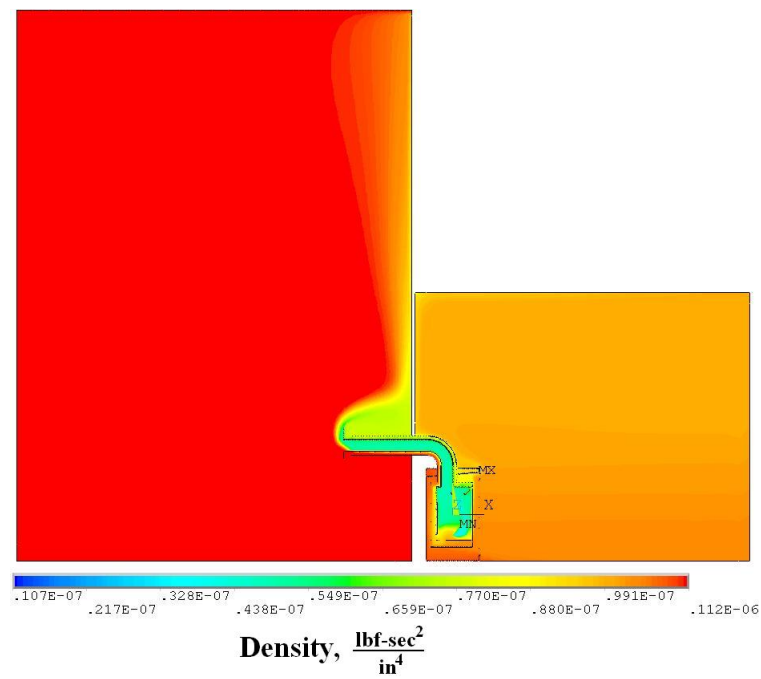


Figure 4.26 2-dimensional fireplace density contour plot

Looking at the temperature contour plot in Figure 4.27, it can now be seen that the temperature solution is indeed affected due to the absence of flow in some sections of the fireplace. It was stated earlier that the flow through the upper portion of the outer duct had been cut off due to the conversion from 3-dimensions to 2-dimensions, as well as the flow through the cavity of air between the outer shell and the inner combustion chamber. Here we can see that the air inside of the upper portion of the outer duct has reached a temperature of over 300°F. This value is much higher than would be seen in the actual fireplace duct. We can also see that from the velocity plots in Figure 4.28 and 4.29 that the flow is virtually stagnant in this duct meaning there is no convective heat transfer which would work to cool the area inside of this duct. These two velocity plots also show that there is no flow through the cavity just inside of the outer shell as was predicted earlier. Due to these discrepancies in airflow and accurate temperature correlation is impossible at these points. The airflow inside of the fireplace is unaffected however, and thus the temperature just outside of the inner glass of the fireplace should be free from spurious results.

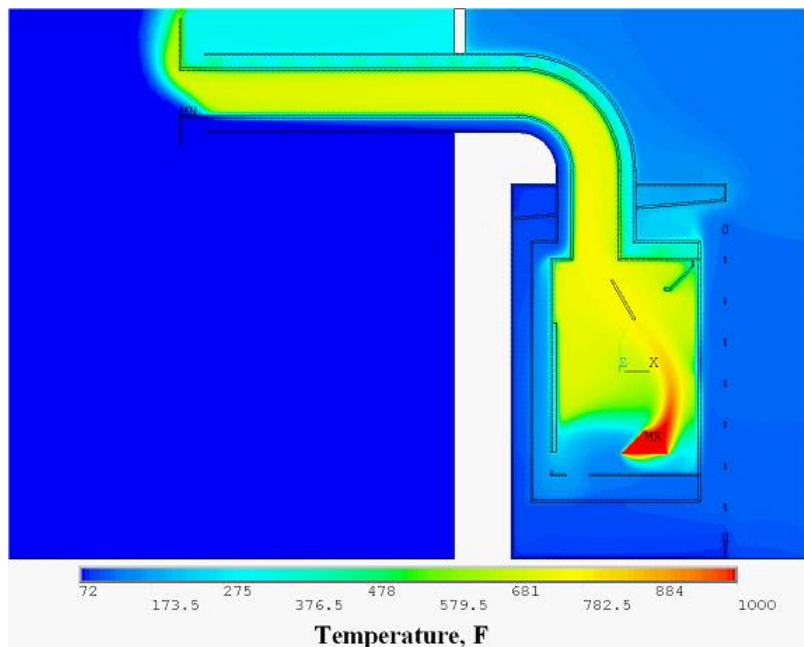


Figure 4.27 Temperature contour plot inside the fireplace

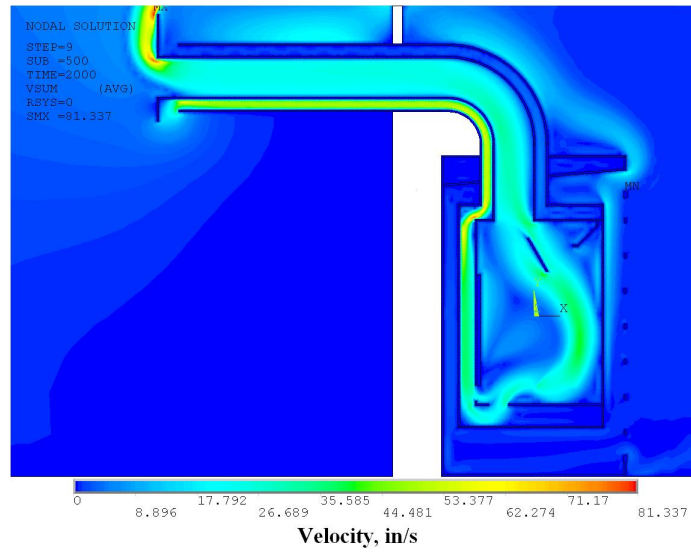


Figure 4.28 Velocity solution inside the fireplace

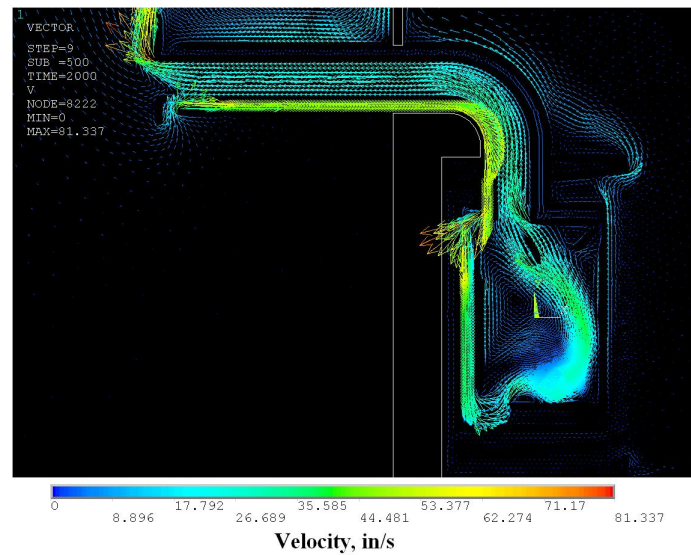


Figure 4.29 Density contour plot inside of the fireplace

The following figure provides a comparison between the glass temperatures for the analytical model and the actual fireplace. Here, the black values are those obtained from the ANSYS solution, and the values in red are those provided by the fireplace manufacturer.

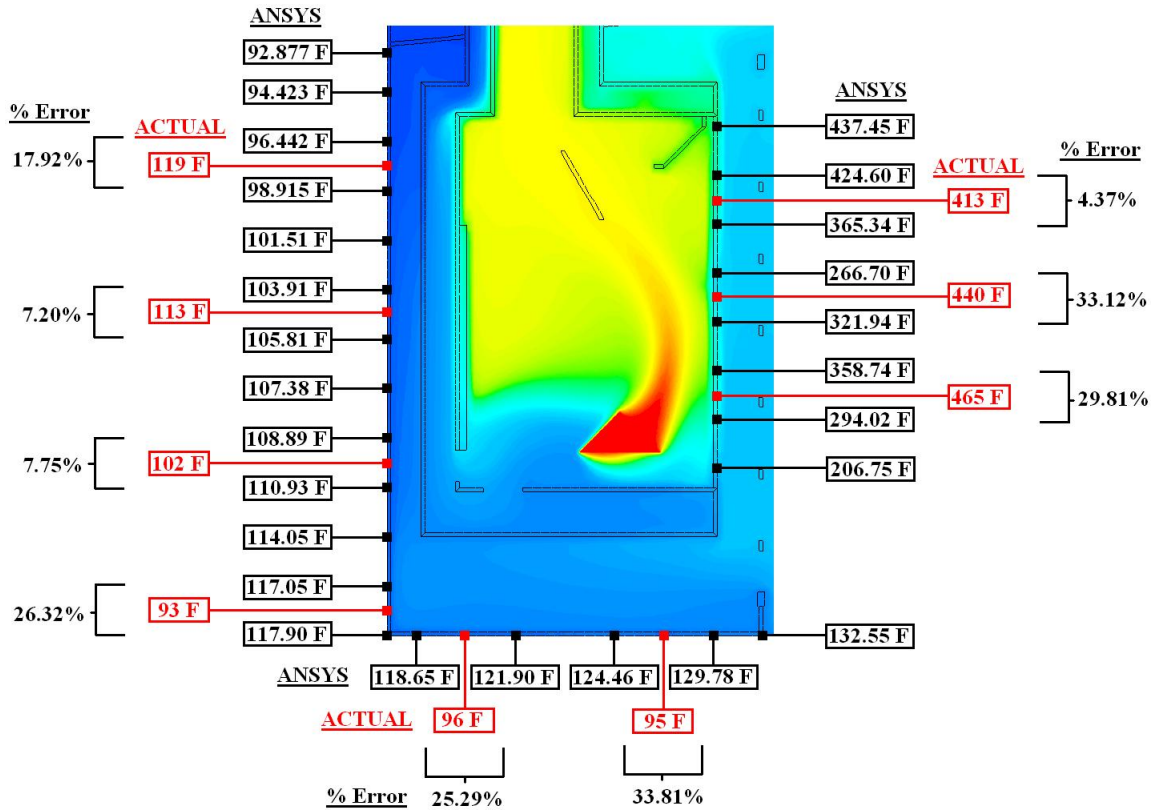


Figure 4.30 Temperature comparison of the inner glass (1000°F)

Figure 4.30 reveals that the temperatures on the outside surface of the inner glass and the floor are actually much lower than they should be. This is most likely due to the selection of the heat source for this model. Here, an arbitrarily shaped heating source was set at a constant 1000°F. This value is actually much lower than the suggested maximum flame temperature for propane which has been calculated to be as high as 3600°F(9). This however is assuming optimum conditions with an ideal amount of air available for combustion. To see how an increase in flame temperature would affect these temperature values on the glass, another simulation was performed with the flame temperature set to the optimum value of 3600°F. The results of that simulation are shown below.

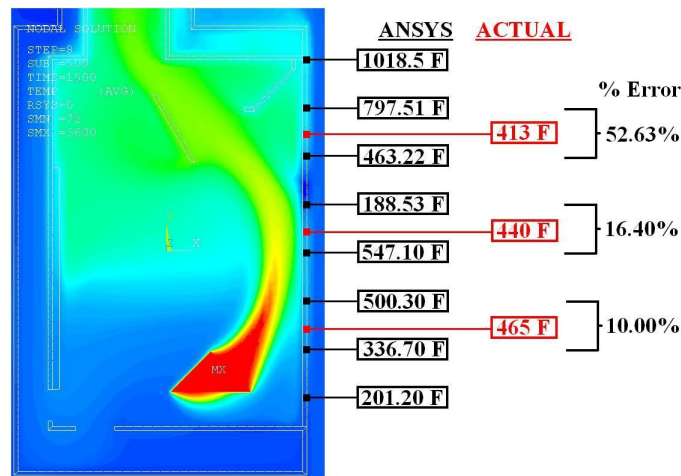


Figure 4.31 Temperature comparison of the inner glass (3600°F)

Figure 4.31 shows that the optimum value of 3600°F for the heating element results in glass temperatures that are now higher than the values obtained through experimental analysis. While, it does provide a closer approximation to the actual temperature values however, these temperatures are still outside of an acceptable range of error. This could be due to many factors, but is most likely a result of the heating element. It is difficult to accurately model a heat source such as this. Simply setting the flame temperature on an area as was done in these simulations may not be accurately representing the amount of heat that is being added into this system. Perhaps a better method would be to model this heating element as a heat generating body. Here, a known heat generation rate is applied over a volume (or area in 2-dimensions). The energy is then passed into the system and the temperatures for the system are calculated from this known value of heat. This however can prove to be difficult as the size of this volume or area is really unknown. While it is possible to force this heat source to generate the proper amount of energy/time (25000 BTU/hr for this fireplace), if the heat source is incorrectly sized the temperatures emitted from this source will drastically increase or decrease. For instance, if the heating source is made to be too small, the average heat generation rate on each area will have to be much higher in order to generate the same amount of heat as a larger heat source. With an increased concentration of heat entering the system one can expect the temperatures of the system around the heating element to increase as well.

This increased temperature results in increase velocities at the heat source as well as decreased pressure, effectively changing the flow of the system completely. Most likely, the best solution to this problem is to reduce the heating element down to a macroscopic scale. Propane gas is known to release approximately $2300\text{BTU}/\text{ft}^3$ during combustion (9). If a person is able to measure the amount of propane combusted at each flame location inside the fireplace precisely (there are multiple flames of varying sizes), then perhaps an accurate representation of the heating element for this fireplace could be modeled. The burner pan for this fireplace is shown below.

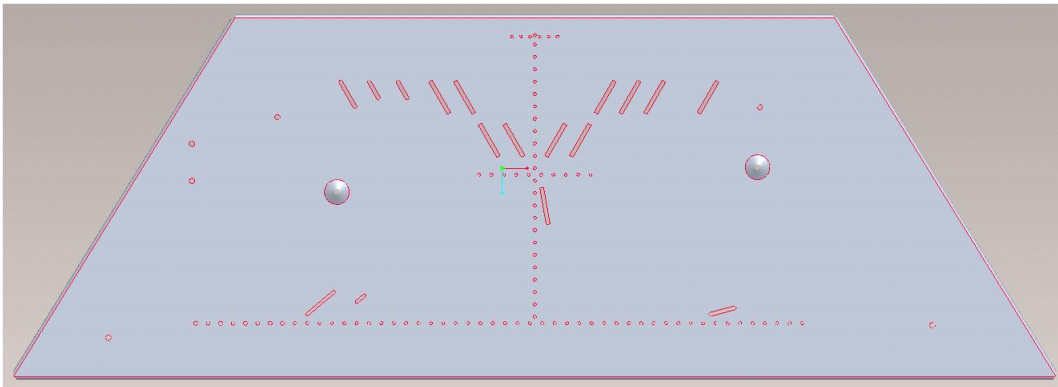


Figure 4.32 Flame locations for the fireplace burner pan

In this figure, each red outlined dot that can be seen on the burner pan represents a location where a flame is sustained. If the rate of propane combustion can be calculated at each of these locations then a rate of energy generation can be calculated and assigned to each location and a much more accurate model could be created for the heat element. However, this model would only be useful for a 3-dimensional model.

CHAPTER 5. Conclusions

The Finite Element analysis results presented in this document have shown that, despite many simplifications as well as flow discrepancies created when converting to 2-dimensions, the temperatures in and around the fireplace are still surprisingly close. While there are some areas where the temperatures vary by a great deal, the overall pattern of temperature distribution appears to accurately reflect that of the actual fireplace. As a move to 3-dimensions is made, the inaccuracies of the 2-dimensional model will be eliminated and these temperatures will be seen to approach those of the actual fireplace. A better method of modeling the heat source must be found however, and an approach similar to that presented in the latter portion of Chapter 4 should be incorporated. Also, if an approximation to the heat loss inside of the room through the walls can be found, the elevated temperatures inside the room will also be seen to decrease and more closely reflect those in an actual room setting.

BIBLIOGRAPHY

- [1] Lewis, Ronald W., Nithiarasu, Perumal and Seetharamu, Kankanhalli N., *Fundamentals of the Finite Element Method for Heat and Fluid Flow*, Wiley, 2004
- [2] Moran, Michael J. and Shapiro, Howard N., *Fundamentals of Engineering Thermodynamics*, 5th Edition, McGraw Hill, 2004
- [3] Anderson Jr., John D., *Fundamentals of Aerodynamics*, 3rd Edition, McGraw Hill, 2001
- [4] Powers, David L., *Boundary Value Problems*, 4th Edition, Harcourt Academic Press, 1999
- [5] Tritt, Terry M., *Thermal Conductivity: Theory, Properties, and Applications*, Kluwer Academic/Plenum Publishers, 2004
- [6] "Chapter 7: Fluid Flow", *ANSYS V11.0 User's Manual*, pg. 1-5, 2007
- [7] "Hot Dip Galvanized Steel", 07/2007, <http://www.aksteel.com/pdf/markets-products/carbon/HotDipGalvanized.pdf>
- [8] "Aluminized Steels", 07/2007, <http://www.aksteel.com/pdf/markets-products/carbon/AlumT1.pdf>
- [9] Guyer, Eric C., *Handbook of Applied Thermal Design*, Taylor & Francis, 1999